Chapter 17

LARGE BASIN RUNOFF MODEL

Thomas E. Croley II

Great Lakes Environmental Research Laboratory
Ann Arbor, Michigan

ABSTRACT

Large-scale watershed models are required to estimate basin runoff to the Great Lakes and other large-basin applications for use in long-term routing determinations, water resource operation decisions, operational hydrology studies, and long-term forecasting. Data availability over large areas, large-basin applicability, computation requirements, and model application costs often preclude the use of detailed watershed models, designed for small scales, for large-scale applications. An interdependent tank-cascade model is described that uses a mass balance coupled with linear reservoir concepts. It is physically based and uses climatological considerations not possible for small watersheds; analytical solutions are employed to bypass numerical inaccuracies. Snowmelt and net supply computations are separable from the mass balance determinations and are based on simple degree-day empiricism. Partial area concepts are used to determine infiltration and surface runoff. Losses are determined from joint consideration of available energy for actual and potential evapotranspiration and of available moisture in the soil horizons by using climatological concepts. Heuristic calibration procedures are described that give insight into the use of the model. The model is applied in example watersheds and it and its calibration are evaluated. Source code, executable programs, and all examples are available in appendices and over the World Wide Web.

17.1. INTRODUCTION

Agencies concerned with managing the water resources of large watersheds, particularly over large time intervals, must be able to assess the expected hydrology of the area. Large-scale watershed models are required for the Laurentian Great Lakes for a variety of purposes and the Great Lakes Environmental Research Laboratory (GLERL) built an appropriate model of large basin runoff. The model was designed as a continuous-time flow representation for assessing water resource questions over the long term (as opposed to, say, flood prediction over the short term). The model must have limited-data requirements, mandated by the limited data availability for large areas such as the Great Lake basins. Allowable data inputs are limited to daily precipitation and air temperature. Also allowed are any data that can be abstracted easily from available maps or climatic summaries. It is also desired that the model concepts be physically based, so that understanding of watershed response to natural forces is facilitated, and the model is economical to use. (The model is applied to 121 basins in the Great Lakes area and the integrated response used in simulation studies and in forecasting of water levels on the lakes.)

During the initial phases of work on the Large Basin Runoff Model (for use in Great Lakes applications), two existing physically-based conceptual models (cascades of storage "tanks") were evaluated for simulating the detailed hydrologic response of individual watersheds. The U.S. Corps of Engineer's Streamflow Synthesis and Reservoir Regulation model (SSARR) and the National Weather Service Hydrologic model (NWSH) were evaluated in terms of reproducing volumes of runoff from the Genesee River Basin in New York State (Potok, 1980). The SSARR model was then used to simulate runoff from the southeast Lake Michigan basin (Derecki and Potok, 1979). These models, particularly the SSARR model, showed potential for use in simulating or forecasting runoff into the Great Lakes. However, they require many parameter determinations, which hinders their physical relevance and makes them expensive to fit. They require too much data in an area where only daily precipitation and temperature are available over large areas. They are expensive to use and therefore their effectiveness depends upon the ability to group watersheds of similar hydrologic characteristics into a single regional "equivalent" watershed. Unfortunately, the application of such lumped-parameter models to very

large areas must necessarily fail to represent areal distributions of watershed and meteorological characteristics.

This chapter presents an interdependent "tank cascade" model that has been tested on the watersheds of the Great Lakes. It was developed from large-scale (climatological) concepts and designed for weekly or monthly volumes of runoff. The model consists of water and heat balances, as do other water-budgeting models, but with alternative physical interpretations given to its components. The model is physically based and uses climatological considerations not possible with small watersheds. In particular, evapotranspiration losses for large areas may now be considered as a function of readily available data. Analytical solutions are presented in favor of numerical solutions to by pass associated numerical error. The calibration procedure developed for use of this model is given, along with an illustration of its use, and evaluated. Program code and executables and all examples are available in appendices on this book's accompanying compact disc and also over the World Wide Web at:

http://www.glerl.noaa.gov/wr/lbrmexamples.html.

17.2. TANK CASCADE MODELS

The mass balance on a watershed is shown in Fig. 17.1 (Croley, 1983a); as shown there, precipitation enters the snow pack, if present, and is then available as snowmelt depending mainly on air temperature and solar radiation.

Snowmelt and rainfall partly infiltrate into the soil and partly run off directly to rivers, depending upon the moisture content of the soil. Infiltration is high if the soil is dry, and surface runoff is high if the soil is saturated.

Soil moisture evaporates or is transpired by vegetation depending upon the types of vegetation, the season, solar radiation, air temperature, humidity, and wind speed. The remainder percolates into deeper basin storages that feed the rivers and lakes through interflows and groundwater flows. Generally, these river supplies are high if the soil and groundwater storages are large. Because of this buffering effect of the large snow pack and the large soil, groundwater, and surface storages, runoff from rivers can remain high for many weeks or even months after high precipitation has stopped.

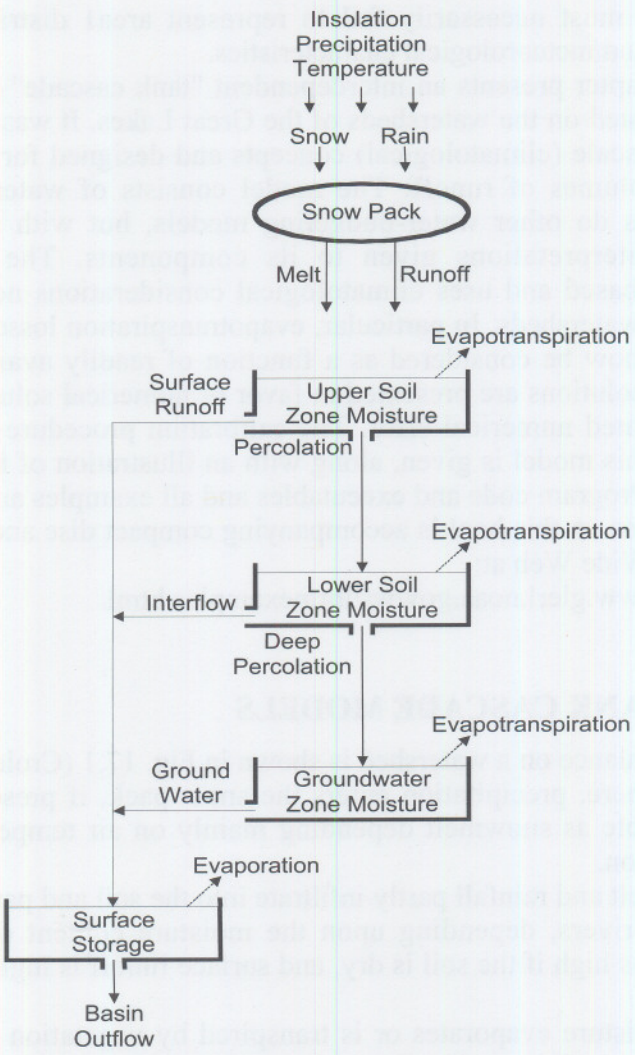

Fig. 17.1. Watershed component tank cascade mass balance.

There are many conceptual models of watershed hydrology that use the "tank cascade" concept, wherein one component of the watershed drains into other components. The Stanford Watershed Model (Crawford and Linsley, 1966) and its many derivatives (including the SSARR and NWSH models) are well-known examples. In these earlier

developments, relationships between various components in the watershed (e.g., surface storage, interception storage, upper and lower soil zones, groundwater storage, and channel storage) are described with classical equations of evaporation, infiltration, and inter-tank flows. Solution of these equations often proceeds numerically with accounting-type calculations. Many variations on the tank cascade concept are included to simulate nuances observed in nature. For example, sometimes minimum storage volumes must be filled in various tanks before any inter-tank flows are allowed; this corresponds to satisfaction of interception and surface depression storage, and of groundwater and soil zone storages above which runoff can occur. Other nuances pertain to satisfaction of evaporation before infiltration and similar flows are allowed. While these variations allow better matching of peak flow rates, they introduce complexities that prohibit analytical solutions, requiring instead that numerical solutions proceed in small time steps. These variations appear unnecessary for volumetric determinations over large time periods (as opposed to finding peak flow rates), and they introduce many parameters to be determined in model calibration. It is difficult to use these models in practical applications because of their extensive data or calibration/optimization requirements, which can become excessive for applications over large areas like the Great Lakes basins.

The tank cascade concept has also been applied in a series of models to determine total runoff hydrographs from very limited data (Edson, 1951; Kalinin and Miljukov, 1958; Nash, 1959, 1960; WMO, 1975). In these applications, many variations to the concept, mentioned above, are not included so that the solution is analytically tractable. They are useful for determining runoff hydrographs; monthly runoff estimates are possible also, presupposing that adequate data are available for determining snowmelt and evapotranspiration. The absence of constraints on tank interflow allows efficient parameter estimation techniques to be employed in some practical applications (Tingsanchali and Loria, 1981).

17.3. DESCRIPTION OF RUNOFF MODEL

In light of the requirements for the large watershed model, where weekly or monthly runoff volumes from large areas are required, the GLERL Large Basin Runoff Model (LBRM) was defined as an

interdependent tank-cascade model by using physical concepts corresponding to Fig. 17.1 (Croley, 1983a, b). The main mathematical feature of this arrangement is that it may be described by strictly continuous equations; none of the complexities associated with inter-tank flow rate dependence on partial filling are introduced. For a sufficiently large watershed, these nuances are not observed due to the spatial integration of the rainfall, snowmelt, and evapotranspiration processes. Since the solution is analytically tractable, large time steps may be employed without introducing numerical error or excessive computational requirements. The integration of data inputs over large time steps may introduce errors that can only be assessed by example applications in the selection of the appropriate time step. However, for large watershed areas, there is some temporal integration of inputs that may make the approximation of uniform inputs over each time interval inconsequential.

In Fig. 17.1, daily precipitation, temperature, and insolation (the latter available from meteorological summaries as a function of location) may be used to determine snowpack accumulations and net supply. The net supply is divided into surface runoff and infiltration to the upper soil zone in relation to the upper soil zone moisture content (U). Percolation to the lower soil zone and evapotranspiration are also dependent on U. Likewise, interflow from the lower soil zone to the surface, evapotranspiration, and deep percolation to the groundwater zone depend on the lower soil zone moisture content (L). Groundwater flow and evapotranspiration from the groundwater zone depend on the groundwater zone moisture content (G). Finally, basin outflow and evaporation from the surface storage (S) depend on its content. Additionally, evaporation and evapotranspiration are dependent on potential evapotranspiration as determined by joint consideration of the available moisture and the heat balance over the watershed.

The upper soil zone is the void space in the surface soil layer to a depth that can be considered to control infiltration, usually a few centimeters. The lower soil zone is located beneath the upper soil zone and above the water table. The groundwater zone is located beneath the water table. These definitions are inexact since the water table fluctuates in time, implying that these zones are not static. Likewise, all moisture in these zones may not be involved in basin outflow. For example, moisture beneath the water table is part of the groundwater zone only if it is part of the flow toward the stream channel network on the watershed surface. Moisture that flows from the watershed as

groundwater movement is not considered part of this groundwater zone. (No provision is made for water flowing in or out of the watershed as groundwater.) While the location and extent of these zones may be poorly defined, conceptually they are zones that give rise to flow rates as pictured in Fig. 17.1.

A more classical approach to watershed hydrology with a tank cascade model would eliminate the surface storage "tank" in Fig. 17.1. The summation of surface runoff, interflow, and groundwater would then constitute basin outflow. This is the concept used in hydrograph separation techniques, such as that given by Barnes (1940) where each component of outflow recession is defined as coming from its respective storage. The schematic of Fig. 17.1 is more appealing since outflow components enter into the channel network before appearing at the basin outflow point.

17.3.1. Net Supply

Precipitation falling onto the watershed surface and snowmelt constitute the net supply to the watershed. Interception can be considered as part of evapotranspiration and surface depression storage is too transient for consideration since peak flow rates are not of interest. Both are well within the error of measurement for average area1 precipitation and are neglected.

Snow accumulation is governed by the concept that precipitation under warm air temperatures occurs as rainfall and under cold temperatures as snow or ice, which accumulates in the snow pack. Snow accumulation is thus governed by the following concept:

$$U\frac{d}{dt}P = -m, \qquad T > 0$$
$$= p, \qquad T \le 0 \tag{17.1}$$

where t = time (d), P = equivalent water volume present in the snow pack (m^3), m = snowmelt rate ($m^3 d^{-1}$), p = precipitation rate ($m^3 d^{-1}$), and T = air temperature (°C). Daily air temperature is estimated typically as the average of daily maximum and minimum temperatures. The simplification of allowing melt only during above-zero air temperatures appeared realistic in example comparisons for volumetric determinations over the week or month (Croley, 1982a). Ignoring

evaporation from, and condensation to, the snow pack is justified by the limited data requirements for which the model is designed. The net supply rate is then given as

$$\begin{aligned} s &= p + m, & T > 0 \\ &= 0, & T \le 0 \end{aligned} \tag{17.2}$$

where s = net supply rate ($m^3 d^{-1}$). Snowmelt is determined from the simple concept that there are no heat additions from which melt could later occur during periods of sub-zero air temperatures. For periods of above-zero air temperatures, snowmelt results from absorbed insolation and precipitation. However, it is constrained by the available snow pack,

$$\begin{aligned} m &= m_p, & m_p d \le P_0, \\ &= P_0 / d, & m_p d > P_0 \end{aligned} \tag{17.3}$$

where m_p = daily potential snowmelt rate ($m^3 d^{-1}$)and the zero subscript on snow pack refers to its initial value at the beginning of the day (at time zero). It is given as:

$$\begin{aligned} m_p &= 0, & T \le 0, \\ &= a\,h, & T > 0 \end{aligned} \tag{17.4}$$

where a = proportionality constant for snowmelt per degree-day ($m^3 {}^\circ C^{-1} d^{-1}$]) and h = degree-days per day (°C d d^{-1}), computed as the integral of air temperature with time over those portions of the day when it is positive. Since the fluctuation of air temperature during the diurnal cycle is unknown, a triangular distribution is assumed (to approximate an expected sinusoidal variation) for ease of computation. The resulting expression for degree-days is:

$$\begin{aligned} h &= 0, & T_{max} &\le 0, \\ &= T_{max}^2 / \left(T_{max} - T_{min}\right)/2, & T_{min} < 0 < T_{max}, \\ &= T, & 0 &\le T_{min} \end{aligned} \tag{17.5}$$

where T_{max} = maximum daily air temperature (°C) and T_{min} = minimum daily air temperature (°C). [Note that snowpack heat storage (warming and cooling) are neglected in Eqs. (17.3) - (17.5)].

17.3.2. Infiltration

At any instant, the net supply rate is divided between surface runoff and infiltration. Surface runoff is proportional to the relative size of the contributing "wetted" area of the watershed (partial-area concept), as well as to the net supply rate

$$r = s\frac{A_w}{A} \tag{17.6}$$

$$f = s - r \tag{17.7}$$

where r = surface runoff rate (m^3d^{-1}), A_w = area of wetted contributing watershed portion (m^2), A = area of the watershed (m^2), and f = infiltration rate (m^3d^{-1}). By further approximating the relative size of the contributing area as the relative content of the upper soil zone (a good assumption for a very thin zone), areal infiltration becomes

$$f = s\left(1 - \frac{U}{C}\right) \tag{17.8}$$

where U = volume of water in the upper soil zone (m^3) and C = capacity of the upper soil zone (m^3). Equation (17.8) may be interpreted as indicating that infiltration is proportional to the volume remaining in the upper soil zone. This is the basis for Horton's infiltration-capacity relationship at a point (Croley, 1977, pp. 168-170), although Horton's model uses volume remaining beneath the point (small area), not over a large area. Equation (17.8) also indicates that infiltration is proportional to the net supply rate. This is an areal concept for infiltration that has been empirically verified (Kumar, 1980); it does not work for infiltration at a point, which is better described by infiltration-capacity concepts.

17.3.3. Tank Outflows

Since hydrograph recessions are described successfully by exponential decay relationships (Linsley, Kohler, and Paulhus, 1975, pp. 225-229), the linear reservoir concept is deemed appropriate for describing outflow rates from the various storages within the watershed. The concept describes an outflow rate as proportional to the storage

remaining. It is expanded here to describe basin outflow, percolation, and deep percolation, as well as the traditional descriptions of interflow and groundwater flow. The form of the equation is

$$z = \alpha Z \tag{17.9}$$

where z = outflow rate from a storage ($m^3 d^{-1}$), a = linear reservoir constant (d^{-1}), and Z = volume of water in storage (m^3). In Eq. (17.9) Z is U and a is a_p for z equal to percolation; Z is L and a is a_i or a_d for z equal to interflow or deep percolation, respectively; Z is G and a is a_g for z equal to groundwater flow; and Z is S and a is a_s for z equal to basin outflow. Small parameter values for a tank outflow imply small releases and large storage volumes; large values imply small storages and outflows nearly equal to inflows. The *half-life* of a tank storage with regard to a specified outflow is defined as the time required for the storage volume to drop to half its initial value in the absence of tank inflows and other outflows. Note, continuity on a tank with no inflows and no other outflows becomes

$$\frac{dZ}{dt} = -z \tag{17.10}$$

By substituting Eq. (17.9) into Eq. (17.10) and solving,

$$Z_t = Z_0 e^{-\alpha t} \tag{17.11}$$

where the subscript denotes time. Substituting $Z_t = (1/2)Z_0$ into Eq. (17.11) yields the half-life:

$$t_h = \frac{\ln 2}{\alpha} \tag{17.12}$$

where t_h = half-life (d). This is an alternate way of expressing the linear reservoir coefficient that allows easier interpretation of coefficient values.

The linear reservoir concept is modified when considering evaporation or evapotranspiration (evaporation plus transpiration) from any zone of the watershed.

$$e = \beta Z e_p \tag{17.13}$$

where e = evaporation or evapotranspiration rate (m^3d^{-1}), β = partial linear reservoir constant (m^{-3}), and e_p = rate of evaporation or evapotranspiration, respectively, still possible (m^3d^{-1}). In Eq. (17.13), evaporation or evapotranspiration is taken as proportional both to the potential rate, determined from heat balance considerations over the watershed, and to the available water volume (reflecting both areal coverage and extent of supply). This is in agreement with existing climatological and hydrological concepts for evapotranspiration opportunity. In Eq. (17.13), Z is U and β is β_u for e equal to upper zone evapotranspiration, Z is L and β is β_ℓ for e equal to lower zone evapotranspiration, Z is G and β is β_g for e equal to groundwater zone evapotranspiration, and Z is S and β is β_s for e equal to surface zone evaporation.

17.3.4. Mass Balance

By combining Eqs. (17.8), (17.9), and (17.13) with the definitions given above, the one-dimensional mass continuity equation may be written for each zone of the watershed (tank). (See Fig. 17.1.)

$$\frac{d}{dt}U = s\left(1 - \frac{U}{C}\right) - \alpha_p U - \beta_u e_p U \tag{17.14}$$

$$\frac{d}{dt}L = \alpha_p U - \alpha_i L - \alpha_d L - \beta_\ell e_p L \tag{17.15}$$

$$\frac{d}{dt}G = \alpha_d L - \alpha_g G - \beta_g e_p G \tag{17.16}$$

$$\frac{d}{dt}S = s\frac{U}{C} + \alpha_i L + \alpha_g G - \alpha_s S - \beta_s e_p S \tag{17.17}$$

In each case, mass continuity yields a first-order linear differential equation of the general form

$$dZ + (\sum \alpha) Z\, dt = g(t)dt \tag{17.18}$$

where $(\sum \alpha)$ = sum of linear reservoir constants on storage for all outflows for the tank and $g(t)$ = sum of time-dependent inflows into the storage. The general solution may be obtained from standard procedures (Rainville, 1964, pp. 36-39)

$$Z_t = e^{-(\sum \alpha)t}\left[Z_0 + \int_0^t g(u)\, e^{(\sum \alpha)u} \partial u\right] \tag{17.19}$$

where the subscript is time. Since data on precipitation and temperature are available only in time increments of a day or larger, the solutions to Eqs. (17.13) – (17.17) are given here by assuming that the net supply and potential evapotranspiration are distributed uniformly over the time increment. Storage values at the end of the time increment are computed from values at the beginning. In the analytical solution, results from one storage zone are used in other zones where their outputs appear as inputs. There are several different solutions, depending upon the relative magnitudes of all coefficients in Eqs. (17.14) - (17.17). As an example, the equations are solved for the daily time increment ($0 < t < d$)

$$U_d = \left(U_0 - \frac{s}{\phi_B}\right)e^{-\phi_B d} + \frac{s}{\phi_B} \tag{17.20}$$

$$L_d = \left(L_0 - \frac{\phi_A}{\phi_D - \phi_B} - \frac{\phi_C}{\phi_D}\right)e^{-\phi_D d} + \frac{\phi_A}{\phi_D - \phi_B} e^{-\phi_B d} + \frac{\phi_C}{\phi_D} \tag{17.21}$$

$$\begin{aligned} G_d = &\left(G_0 - \frac{\phi_E}{\phi_H - \phi_D} - \frac{\phi_F}{\phi_H - \phi_B} - \frac{\phi_G}{\phi_H}\right)e^{-\phi_H d} \\ &+ \frac{\phi_E}{\phi_H - \phi_D} e^{-\phi_D d} + \frac{\phi_F}{\phi_H - \phi_B} e^{-\phi_B d} + \frac{\phi_G}{\phi_H} \end{aligned} \tag{17.22}$$

$$\begin{aligned} S_d = &\left(S_0 - \frac{\phi_L}{\phi_P - \phi_H} - \frac{\phi_M}{\phi_P - \phi_D} - \frac{\phi_N}{\phi_P - \phi_B} - \frac{\phi_O}{\phi_P}\right)e^{-\phi_P d} \\ &+ \frac{\phi_L}{\phi_P - \phi_H} e^{-\phi_H d} + \frac{\phi_M}{\phi_P - \phi_D} e^{-\phi_D d} + \frac{\phi_N}{\phi_P - \phi_B} e^{-\phi_B d} + \frac{\phi_O}{\phi_P} \end{aligned} \tag{17.23}$$

where

$$\phi_B = \frac{s}{C} + \alpha_p + \beta_u e_p \tag{17.24}$$

$$\phi_A = \alpha_p \left(U_0 - \frac{s}{\phi_B} \right) \tag{17.25}$$

$$\phi_C = \alpha_p \frac{s}{\phi_B} \tag{17.26}$$

$$\phi_D = \alpha_i + \alpha_d + \beta_\ell e_p \tag{17.27}$$

$$\phi_E = \alpha_d \left(L_0 - \frac{\phi_A}{\phi_D - \phi_B} - \frac{\phi_C}{\phi_D} \right) \tag{17.28}$$

$$\phi_F = \frac{\alpha_d}{\phi_D - \phi_B} \phi_A \tag{17.29}$$

$$\phi_G = \alpha_d \frac{\phi_C}{\phi_D} \tag{17.30}$$

$$\phi_H = \alpha_g + \beta_g e_p \tag{17.31}$$

$$\phi_L = \alpha_g \left(G_0 - \frac{\phi_E}{\phi_H - \phi_D} - \frac{\phi_F}{\phi_H - \phi_B} - \frac{\phi_G}{\phi_H} \right) \tag{17.32}$$

$$\phi_M = \frac{\alpha_g}{\phi_H - \phi_D} \phi_E + \frac{\alpha_i}{\alpha_d} \phi_E \tag{17.33}$$

$$\phi_N = \frac{\alpha_g}{\phi_H - \phi_B} \phi_F + \frac{\alpha_i}{\alpha_d} \phi_F + \frac{s}{C} \frac{\phi_A}{\alpha_p} \tag{17.34}$$

$$\phi_O = \alpha_g \frac{\phi_G}{\phi_H} + \frac{\alpha_i}{\alpha_d}\phi_G + \frac{s}{C}\frac{\phi_C}{\alpha_p} \tag{17.35}$$

$$\phi_P = \alpha_s + \beta_s e_p \tag{17.36}$$

The subscripts 0 and d on the storage volumes represent the beginning and the end of the day, respectively. This solution applies for the case where $\phi_D \neq \phi_B$, $\phi_H \neq \phi_D$, $\phi_H \neq \phi_B$, $\phi_P \neq \phi_H$, $\phi_P \neq \phi_D$, $\phi_P \neq \phi_B$, $\phi_B \neq 0$, $\phi_D \neq 0$, $\phi_H \neq 0$, $\phi_P \neq 0$, $C \neq 0$, $\alpha_p \neq 0$, and $\alpha_d \neq 0$. As long as α_p, α_i, α_g, α_s, and C are non-zeros, then there are 30 possible analytical results, depending upon the values of ϕ_B, ϕ_D, ϕ_H, ϕ_P, and α_d: 15 for $\alpha_d = 0$ and 15 for $\alpha_d \neq 0$. (See Fig. 17.2.) Since these quantities (ϕ_B, ϕ_D, ϕ_H, and ϕ_P) involve the variables s and e_p, which change from day to day, then the appropriate analytical result, as well as its solution, varies with time. Mathematical continuity between solutions is preserved however. These results are summarized elsewhere (Croley, 1982a). A watershed model must have all solution possibilities present for effective implementation.

The flow volumes over any time increment may then be determined directly since outflow volumes are related by their ratio of linear reservoir coefficients.

$$V_s = \int_0^d s\,dt = s\,d \tag{17.37}$$

$$V_r = \left(V_s + U_0 - U_d\right)\frac{s}{C}\frac{1}{\phi_B} \tag{17.38}$$

$$V_f = V_s - V_r \tag{17.39}$$

$$V_p = \left(V_s + U_0 - U_d\right)\frac{\alpha_p}{\phi_B} \tag{17.40}$$

$$E_u = \left(V_s + U_0 - U_d\right)\frac{\beta_u e_p}{\phi_B} \tag{17.41}$$

$$V_i = \left(V_p + L_0 - L_d\right)\frac{\alpha_i}{\phi_I} \tag{17.42}$$

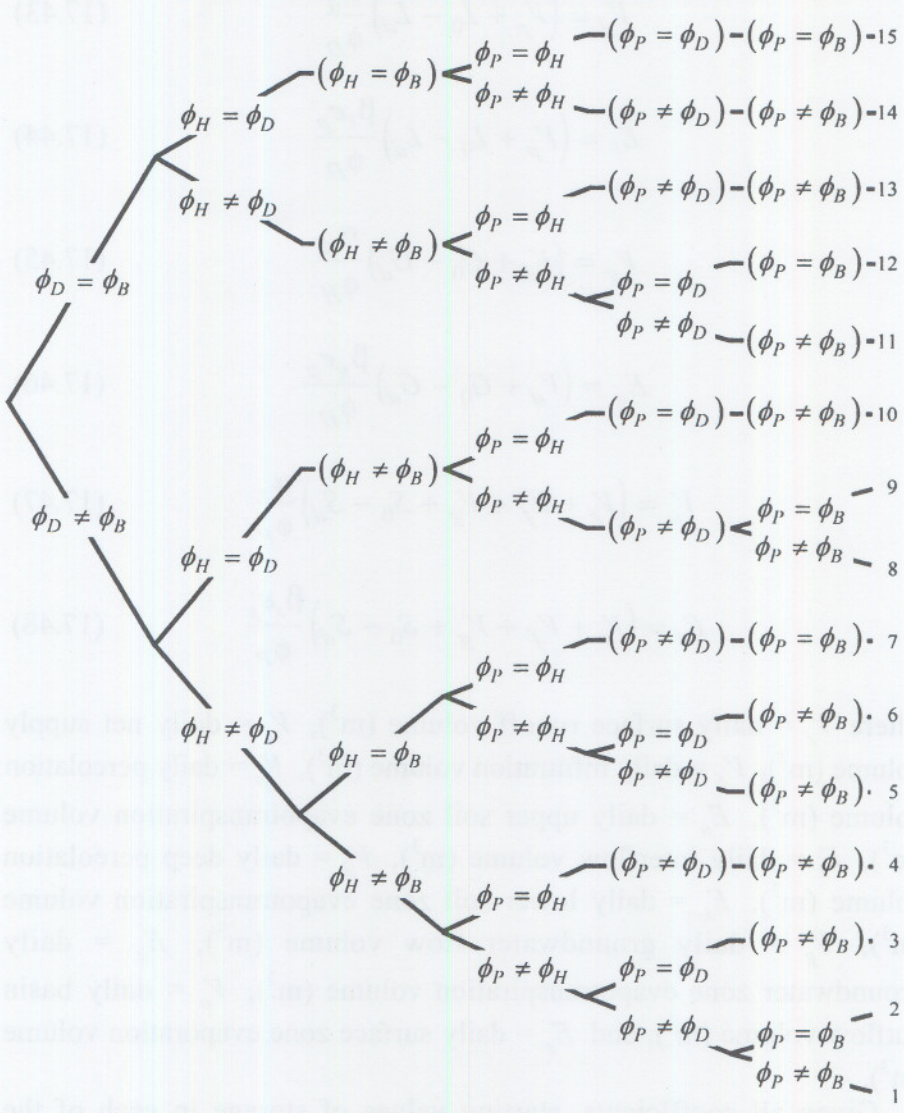

Fig. 17.2. Analytical solution possibilities.

$$V_d = \left(V_p + L_0 - L_d\right)\frac{\alpha_d}{\phi_D} \tag{17.43}$$

$$E_\ell = \left(V_p + L_0 - L_d\right)\frac{\beta_\ell e_p}{\phi_D} \tag{17.44}$$

$$V_g = \left(V_d + G_0 - G_d\right)\frac{\alpha_g}{\phi_H} \tag{17.45}$$

$$E_g = \left(V_d + G_0 - G_d\right)\frac{\beta_g e_p}{\phi_H} \tag{17.46}$$

$$V_o = \left(V_r + V_f + V_g + S_0 - S_d\right)\frac{\alpha_s}{\phi_P} \tag{17.47}$$

$$E_s = \left(V_r + V_f + V_g + S_0 - S_d\right)\frac{\beta_s e_p}{\phi_P} \tag{17.48}$$

where V_r = daily surface runoff volume (m^3), V_s = daily net supply volume (m^3), V_f = daily infiltration volume (m^3), V_p = daily percolation volume (m^3), E_u = daily upper soil zone evapotranspiration volume (m^3), V_i = daily interflow volume (m^3), V_d = daily deep percolation volume (m^3), E_ℓ = daily lower soil zone evapotranspiration volume (m^3), V_g = daily groundwater flow volume (m^3), E_g = daily groundwater zone evapotranspiration volume (m^3), V_o = daily basin outflow volume (m^3), and E_s = daily surface zone evaporation volume (m^3).

Given all coefficients, starting values of storage in each of the component zones, net supply rate, and potential evapotranspiration rate, the values of (ϕ_B, ϕ_D, ϕ_H, and ϕ_P) can be computed from Eqs. (17.24), (17.27), (17.31), and (17.36), respectively. Based upon their values, the appropriate analytical results [Eqs. (17.25), (17.26), (17.28) – (17.30), and Eqs. (17.32) – (17.35)] are used to compute the remaining

intermediate values. The appropriate analytical solution [e.g., Eqs. (17.20) – (17.23) for ϕ_B, ϕ_D, ϕ_H, and ϕ_P all different and non-zero and $\alpha_p \neq \upsilon$] is then used to compute the end-of-day storage values (which become the beginning-of-day values for the next day). Finally, daily flow volumes can be obtained from Eqs. (17.37) – (17.48).

The analytical solutions of Eqs. (17.14) – (17.17) are "continuous"; that is they are amenable to ordinary solution techniques. Furthermore, solutions may proceed for either flow rates or storage volumes directly without the complication of constraint consideration. All derivatives of the solutions with respect to individual parameters exist and are continuous; therefore, analytical gradient-search procedures are possible in parameter determination. The solutions are physically satisfying; non-negative flow rates and storage volumes are guaranteed with any physically plausible set of inputs. The solution equations are unchanged for other time increments; the daily time interval, d, would be simply replaced in the equations. The net supply and potential evapotranspiration are considered to be uniform over the time interval and the choice of time interval must assess the validity of this treatment.

17.3.5. Evapotranspiration

All incoming heat is considered here to be released by the watershed surface by ignoring heat storage and the energy advected by evaporation. The release consists of atmospheric heating (composed of short-wave reflection, net long wave exchange, sensible heat exchange, net atmospheric advection, and net hydrospheric advection), snowmelt and evaporation-evapotranspiration (referred to herein jointly as evapotranspiration). At any instant, the evapotranspiration rate is proportional to the amount of water available as in Eq. (17.13) (reflecting both areal coverage and extent of supply), and to the rate of non-latent heat released to the atmosphere (atmospheric heating), dH/dt (Croley, 1982b):

$$e_p = \frac{dH}{dt} \Big/ (\rho_w \gamma_v) \qquad (17.49)$$

where γ_v = latent heat of vaporization (596 - 0.52 T cal g^{-1}) and ρ_w = density of water (10^6 g m^{-3}). Potential evaporation is the evaporation that would occur if adequate moisture were available. It is often taken as

the amount expected from an open water surface and is used as an estimate of potential evapotranspiration over land and vegetative surfaces (Gray, 1973, pp. 339-353). Very often, engineering calculations of potential evapotranspiration use climatic indicators of temperatures, wind speeds, humidities, etc., by assuming that these quantities are independent of the actual evapotranspiration that does occur. This is adequate for estimates over small areas where evapotranspiration has only a small effect on these quantities. However, over a large area, climatological observations suggest that actual evapotranspiration affects these quantities and hence affects potential evapotranspiration (evapotranspiration opportunity or capacity); the heat used for evapotranspiration reduces the opportunity for additional evapotranspiration (complementary evapotranspiration and evapotranspiration opportunity concept). Morton (1965) made use of this concept to compute regional evapotranspiration from climatological observations. Witherspoon (1970) used an approximation of Morton's work to compute basin evapotranspiration in a volumetric flow model for Lake Ontario. Bouchet (1963) postulated that the potential evapotranspiration energy is the absorbed insolation less the energy used for regional evapotranspiration.

This concept is modified here for use on a smaller-than-regional scale by considering that a portion of the net heat balance after absorbed insolation is available for either potential or actual evapotranspiration. That is, part of it is used in evapotranspiration and the rest of it determines the potential evapotranspiration. Thus, the total heat available for evapotranspiration over a day is composed of the heat actually used for evapotranspiration and that used for atmospheric heating.

$$\Psi = H + \rho_w \gamma_v \left(E_u + E_\ell + E_g + E_s \right) \qquad (17.50)$$

where Ψ = total heat available for evapotranspiration during the day (cal) and H = non-latent heat released to the atmosphere during the day (cal). The value of e_p is determined by simultaneous solution of Eqs. (17.14) – (17.17) and the following complementary relationship between actual evapotranspiration and that still possible from atmospheric heat, derived from Eq. (17.49) and Eq. (17.50):

$$\int_0^d \left[e_p + \left(\beta_u U + \beta_\ell L + \beta_g G + \beta_s S \right) e_p \right] dt = \Psi / \left(\rho_w \gamma_v \right) \quad (17.51)$$

The evaporation from stream channels and other water surfaces (surface zone) in a large basin is very small compared to the basin evapotranspiration; groundwater evapotranspiration is also taken here as being relatively small. By taking e_p as uniform over the day and ignoring evapotranspiration from the surface and groundwater zones, Eq. (17.51) yields:

$$e_p \cong \frac{1}{d \rho_w \gamma_v} \frac{\Psi}{1 + \beta_u \bar{U} + \beta_\ell \bar{L}} \quad (17.52)$$

where $\bar{U}$ = average water volume in the upper soil zone (m^3) over the day and $\bar{L}$ = average water volume in the lower soil zone over the day (m^3). As expected, both potential and actual evapotranspiration depend upon the available water supply. If the water supply is large, actual evapotranspiration approaches the limit of the water supply or $\Psi / \rho_w \gamma_v$ and potential evapotranspiration approaches zero. If the water supply is small, actual evapotranspiration approaches zero and potential evapotranspiration approaches $\Psi / \rho_w \gamma_v$ (Croley, 1982b). The average storages can be computed from the mass balance equations as

$$\bar{U} = \frac{1}{d \alpha_p} \frac{\phi_A}{\phi_B} \left(1 - e^{-\phi_B d} \right) + \frac{\phi_C}{\alpha_p} \quad (17.53)$$

$$\bar{L} = \frac{1}{d \alpha_d} \frac{\phi_E}{\phi_D} \left(1 - e^{-\phi_D d} \right) + \frac{1}{d \alpha_d} \frac{\phi_F}{\phi_B} \left(1 - e^{-\phi_B d} \right) + \frac{\phi_G}{\alpha_d} \quad (17.54)$$

This solution applies for the case $\phi_D \neq \phi_B$, $C \neq 0$, $\alpha_p \neq \upsilon$, and $\alpha_d \neq 0$. As long as C and α_p are non-zero, then for either $\phi_D = \phi_B$ or $\alpha_d = 0$ or both, alternative expressions result (Croley, 1982a). Since e_p is involved in the intermediate variables ϕ_B and ϕ_D, an iterative solution is used to determine e_p each day in the mass balance if Ψ is known.

The determination of Ψ from observable meteorological variables is difficult (recall the limitation to daily precipitation and air temperature). During times of snow cover, e_p is zero with respect to the upper and lower soil zones. Recall, during times of no snow cover, the remainder

of the heat balance on the watershed surface after absorbed insolation consists of short-wave reflection, net long-wave radiation exchange, sensible heat transfer, net hydrospheric and atmospheric advection, latent heat transfer, and energy advected by evaporation. Also recall energy advected by evapotranspiration is small compared to latent heat transfer and is neglected in Eq. (17.51).

Daily air temperature is taken here as an integrated reflection of the portion Ψ of the remaining heat balance after absorbed insolation. This concept is satisfying in that air temperature is considered an indicator of the heat balance, rather than an independent variable in the determination of potential evaporation as is done classically. At low temperatures, it is expected that Ψ is small since potential and actual evapotranspiration are low at low temperatures. Over the daily cycle, this energy is rarely negative (net condensation) and is considered here as strictly positive. The heat available for evapotranspiration is estimated empirically from the average air temperature as follows:

$$\Psi = k \exp\left(T / T_b\right) \tag{17.55}$$

where k = units and proportionality constant (cal), and T_b = a base scaling temperature (°C). [Other empiricisms were eliminated in other studies (Croley, 1982a).] The constant, k, is determinable from the following boundary constraint on the long-term heat balance:

$$\sum \Psi_i = \sum \left(\sigma_i - m_i \rho_w \gamma_f\right) d \tag{17.56}$$

where σ = daily solar insolation at the watershed surface (cal d^{-1}), γ_f = latent heat of fusion (79.7 cal g^{-1}), and the subscript, i, refers to daily values. Equation (17.56) conserves energy in that all insolation not used for snowmelt appears sooner or later as other components of the heat balance that determine Ψ. Daily insolation at the surface of the watershed may be estimated from extraterrestrial radiation and cloud cover:

$$\sigma = 10000 A \tau \left(b_1 + b_2 x\right) \tag{17.57}$$

where τ = daily extra-terrestrial solar radiation (langleys d^{-1}) available in standard climatological summaries as a function of latitude and time of the year, b_1 and b_2 = empirical constants, and x = daily ratio of hours

of bright sunshine to maximum possible hours of bright sunshine, estimated from daily air temperatures (Gray, 1973). In the absence of cloud cover data, x may be estimated (Crawford and Linsley, 1966, p. 50) from

$$x = MIN\left[\left(T_{max} - T_{min}\right)/15,\ 1.0\right] \qquad (17.58)$$

There were several alternatives to the "heat balance" used here to compute snowmelt and evapotranspiration. These were considered early in the model development, but were impeded by the limited-data design objectives. Comprehensive heat balances that considered all advection terms through control volumes defined over the upper soil zone or upper and lower soil zones were written in the early modeling. Net long-wave radiation transfer and sensible heat transfer were estimated directly by using empirical relations. These relations required unavailable data, which were estimated based on engineering judgment. Freezing of the upper soil zone, snowpack and ice formation and decay, and Penmann's potential evapotranspiration were all computed as part of these comprehensive heat balances. The net supply and evapotranspiration models presented here resulted in a two-fold improvement in modeling over these earlier efforts (Croley, 1982a), as measured by the root mean square error of model output (basin outflow). Presumably, these models are superior because of their limited data requirements. Also, the use of air temperatures as an indicator of what has occurred in the watershed is superior to its use as an independent variable in computing potential evapotranspiration and net supply. This change in perspective is fundamental to modeling large-scale watershed hydrology from a climatological viewpoint.

17.4. APPLICATION

The Great Lakes Environmental Research Laboratory developed, calibrated, and verified conceptual model-based techniques for simulating hydrological processes in the Laurentian Great Lakes (including Georgian Bay and Lake St. Clair, both as separate entities). GLERL integrated the models into a system to estimate lake levels, whole-lake heat storage, and water and energy balances for forecasts and for assessment of impacts associated with climate change (Croley,

1990, 1993a,b; Croley and Hartmann, 1987, 1989; Croley and Lee, 1993; Croley et al., 1996, 1998; Hartmann, 1990). During the application process, experience was gained that may benefit others who would apply the LBRM to large basins.

17.4.1. Data Preparation

For application of the LBRM to a very large drainage basin (such as that associated with a Great Lake), the basin is first divided into watersheds with areas of between 120 - 20000 km^2 (there are 121 watersheds in the entire Great Lakes basin); most are between 1000 - 5000 km^2. The following input data are required to apply the model: daily precipitation, daily minimum and maximum air temperatures, a standard climatological summary of daily extraterrestrial solar radiation and empirical constants (b_1 and b_2), and for comparison purposes, daily basin outflows. Conversion of units for precipitation from inches per day or centimeters per day to cubic meters per day and for insolation [see Eq. (17.56)] from langleys per day to calories per day involves the area of the watershed. The meteorological data from stations about and in a watershed are combined through Thiessen weighting to produce areally-averaged daily time series of precipitation and minimum and maximum air temperatures for each watershed. In past determinations of water supply effects from climate change scenarios (Croley, 1990, 1992, 1993a; Croley and Hartmann, 1989; Hartmann, 1990), GLERL used about 1,800 meteorological stations for overland precipitation and air temperature (about 15 per watershed or approximately 1 per 70 km^2). Recent experience (Croley and Hartmann, 1986, 1987; Croley et al., 1996, 1998) also suggests that 5-30 stations per watershed for overland meteorology is sufficient for operation of the LBRM at daily time intervals. Thiessen weights are determined for each day of record, if necessary, since the data collection network changes frequently as stations are added, dropped, and moved or fail to report from time to time. This is feasible through the use of an algorithm for determining a Thiessen area-of-influence about a station by its edge (Croley and Hartmann, 1985). Flow records of all "most-downstream" flow stations are combined by aggregating and extrapolating for ungaged areas to estimate the daily runoff from each watershed. Daily basin outflow is reported in either cubic feet per second or cubic meters per second and is converted to cubic meters per day. Then, the LBRM may be applied

in a "distributed-parameter" application by combining model outflows from each of the watersheds to produce the entire basin runoff.

By combining the meteorological and hydrological data for all watersheds to represent the entire basin, the LBRM also may be calibrated in a "lumped-parameter" application to the entire basin at one time. Although the application of lumped-parameter models to very large areas necessarily fails to represent areal distributions of watershed and meteorological characteristics, spatial filtering effects tend to cancel data errors for small areas as the areas are added together. Distributed-parameter applications, in which the LBRM is calibrated for each watershed and model outflows are combined to represent the entire basin, make use of information that is lost in the lumped-parameter approach; the integration then filters individual watershed model errors.

There are five variables to be initialized prior to modeling: P, U, L, G, and S as P_0, U_0, L_0, G_0, and S_0, respectively. While the initial snow pack, P_0, is easy to determine as zero during major portions of the year, these variables are generally difficult to estimate. If the model is to be used in forecasting or for short simulations, then it is important to determine these variables accurately prior to use of the model. They may be taken as the values at the end of a previous model run, preceding the time period of interest, for forecasting uses of the model. If the model is to be used for calibration or for long simulations, then the initial values are unimportant. The effect of the initial values diminishes with the length of the simulation and after 1 or more years of simulated results, the effects are absent from a practical point of view. Calibrations should be repeated with initial conditions equal to observed long-term averages until there is no change in the averages to avoid arbitrary initial conditions when their effects do not diminish rapidly.

17.4.2. Model Use

There are 30 different analytical results, depending upon the relative magnitudes of the inputs (s), the initial conditions (U_0, L_0, G_0, S_0, P_0), and the model parameters (T_b, a, α_p, β_u, α_i, α_d, β_ℓ, α_g, and α_s) in Eqs. (17.14) – (17.17), as noted earlier. Note that C is taken (arbitrarily) as equivalent to 2 cm over the watershed area. Since a change in C can be exactly compensated for (in terms of intrabasin flows and evapotranspiration) by changes in the other parameters, C is set arbitrarily. However, the magnitude of C affects the magnitudes of all tank storage volumes and should be determined if boundary conditions

on soil moisture (or other storage volumes) are available. Note also that β_g and β_s are taken as zeroes since evaporation from the surface and evapotranspiration from the groundwater zone are small relative to evapotranspiration for the upper and lower soil zones; see Fig. 17.3. Finally, empirical coefficients b_1 and b_2 are taken from available climatological summaries.

GLERL has calibrated the LBRM for each Great Lakes watershed with 30 years of daily weighted watershed climatologic data. The nine parameters are determined (Croley and Hartmann, 1984) by searching the parameter space systematically, minimizing the root mean square error between model and actual outflows for each parameter, selected in rotation, until all parameters converge within two or three significant digits. Comparisons with other runoff models (Croley, 1983a) and climatology (Croley and Hartmann, 1984) show the LBRM to be superior for estimates of runoff volumes from large basins.

The LBRM captures "realism" in its structure that has several advantages over other models. Basin storages, modeled as "tanks," are automatically removed as respective parameters approach their limits. Thus, the structure of the model changes within a calibration. This is achieved without the use of "threshold" parameters in the model since physical concepts are used which avoid discontinuities in the goodness-of-fit as a function of the parameters; these concepts appear especially relevant for large-basin modeling. Because the "tanks" relate directly to actual basin storages, initialization of the model corresponds to identifying storages from field conditions which may be measured; interpretations of a basin's hydrology then can aid in setting both initial and boundary conditions. The tanks in Figs. 17.1 or 17.3 may be initialized to correspond to measurements of snow and soil moisture water equivalents available from aerial or satellite monitoring. Snow water equivalents are used in Lake Superior applications (Gauthier et al., 1984).

17.5. EXAMPLE APPLICATION

The Lake Superior Basin, above the locks at Sault Ste. Marie, drains about 130,000 km^2 of Ontario, Minnesota, Wisconsin, and Michigan. It is divided into 22 watersheds for use with the LBRM (see Fig. 17.4). Watershed boundaries are based on state hydrologic unit maps from the

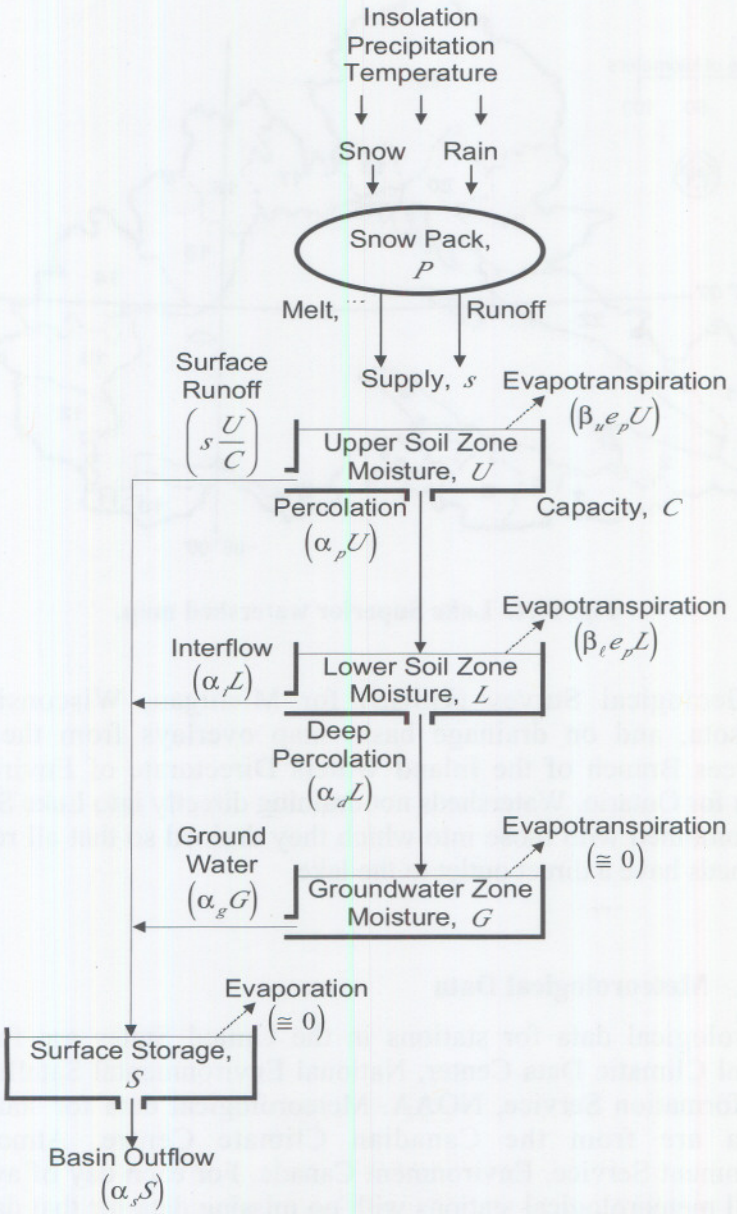

Fig. 17.3. Watershed component tank cascade mass balance.

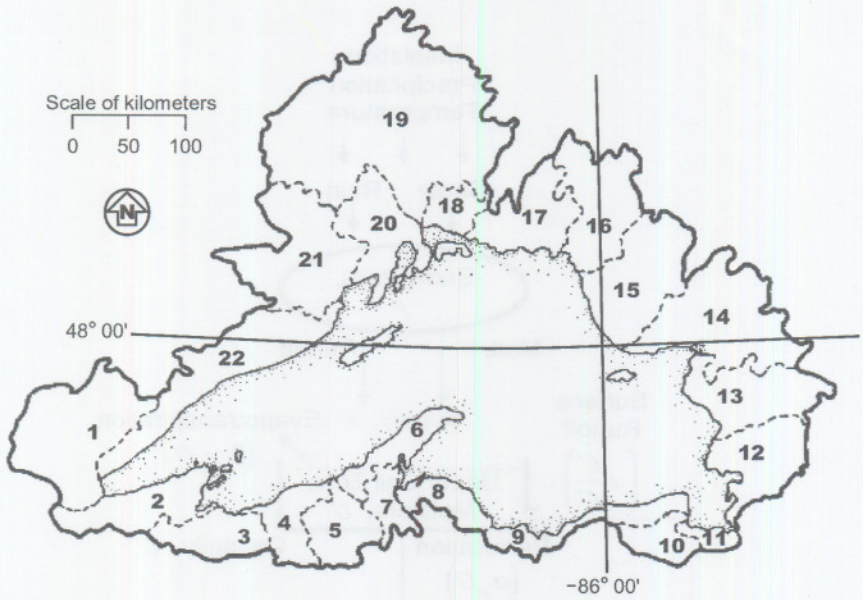

Fig. 17.4. Lake Superior watershed map.

U.S. Geological Survey (USGS) for Michigan, Wisconsin, and Minnesota, and on drainage basin map overlays from the Water Resources Branch of the Inland Waters Directorate of Environment Canada for Ontario. Watersheds not draining directly into Lake Superior were combined with those into which they drained so that all resulting watersheds have a direct outlet to the lake.

17.5.1. Meteorological Data

Meteorological data for stations in the United States are from the National Climatic Data Center, National Environmental Satellite Data and Information Service, NOAA. Meteorological data for stations in Canada are from the Canadian Climate Centre, Atmospheric Environment Service, Environment Canada. For each day of available data, all meteorological stations with no missing data for that day were used to compute all Thiessen weights, which in turn were used to weight available meteorological data to determine daily watershed spatial averages. In the event that no stations have data on a given date, then

the average value of the weighted data on the corresponding day-of-the-year for all available years of record was used to fill in. Thus there are no missing data values (and there must *not* be) in the meteorological data files prepared for use with the LBRM and its calibration. A daily meteorological data set for the entire Lake Superior basin (land area) was constructed by multiplying each areal-average daily data value from each watershed by the corresponding watershed area, summing all weighted values for the entire basin (from all watersheds being used), and dividing by the sum of the drainage areas actually used. The daily meteorological data sets are judged to be very complete; areal-averaged daily air temperatures and precipitation for each watershed are more than 99-percent complete.

17.5.2. Hydrological Flow Data

All "most-downstream" stream flow gages are used with their drainage areas as given by the USGS or Inland Waters Directorate, while the total area in each watershed is based on the state hydrologic unit maps and drainage basin map overlays, discussed previously. Relative drainage areas for all flow gages were determined by dividing each gaged area by the total area of the watershed. All hydrological stations within a given watershed (non-overlapping drainage areas) whose records contain no missing data, for each day in question, were used to determine the watershed outflows into Lake Superior for that day. This aggregation for each day was accomplished by adding data values from each gage within the watershed and dividing by the sum of the relative drainage areas for the gages actually used, to extrapolate for the entire watershed area. Thus, missing data at a given gage were effectively "filled-in" by using data at nearby gages within the same watershed. If no gages in a watershed have data for a given day, then the flow total was set equal to "–9999" to denote missing data. A daily hydrologic data set for the entire Lake Superior basin was constructed by adding extrapolated watershed outflows from each watershed with no missing data for the day in question and dividing by the ratio of the sum of drainage areas of each watershed actually used with respect to the entire basin. The daily hydrological data sets are judged to be very nearly complete; except for watersheds 9 and 11, for which there are no flow data.

17.5.3. Insolation

Values of average mid-monthly daily short-wave radiation received on a horizontal position of the earth's surface under cloudless skies were taken from Gray (1973; pp. 3.11 - 3.16) and used in the following formula, also adapted from Gray (1973):

$$\sigma = 10000 A \tau_s (0.355 + 0.68x) \qquad (17.59)$$

where τ_s = cloudless daily insolation (langleys d^{-1}) interpolated from the average mid-monthly values. Equation (17.59) is similar to Eq. (17.57) where τ_s replaces τ, $b_1 = 0.355$, and $b_2 = 0.68$.

17.5.4. Model Application

The Large Basin Runoff Model is programmed in FORTRAN 95 for (IBM-compatible) personal computers, suitable for use under either MSDOS or Windows (95, 98, NT, or 2000). Appendix A, on the book's companion compact disc for this chapter, contains source code and executables for both versions of the model (DOS or Windows). (All material in the appendices on this book's accompanying compact disc are also available over the World Wide Web at http://www.glerl.noaa.gov/wr/lbrmexamples.html.) Appendices B and C illustrate the use of the LBRM for watershed outflow simulation. Appendix B contains example sets of input files (meteorological data, model parameters, boundary conditions, and input filename list) for Lake Superior watersheds 1 through 22, excluding numbers 9 and 11 (see Fig. 17.4), and for the entire land portion of the Superior basin treated as a single watershed. Appendix C contains the corresponding output files (with end-of-day values for daily runoff, upper soil zone moisture, lower soil zone moisture, groundwater zone moisture, surface zone moisture, and snow pack).

No changes in the source code are required for use of the model on other watersheds. The model is configured dynamically at run time to use sufficient computer memory (if it is available) to store all input files before calculating outputs. This allows speedier processing, particularly during calibration, but requires sufficient memory be available. The file LBRM.F95 in Appendix A, contains the model code; it also contains complete documentation on all input and output files of the model as well as compilation instructions. To use the model, place four files from

Appendix B (e.g., CLMASC01.SUP, PARAM01.SUP, BNDCNDXX.SUP, and LBRM.CFG) and either the DOS-executable or the Windows-executable files of Appendix A into an application directory together. Under either MSDOS or Windows, execute the model code. It first opens and reads the file, LBRM.CFG, to input the filenames it is to use for its input and output files (the above files must be named therein). Then it reads the data, boundary/initial conditions, and parameters files and writes the output file (also named in LBRM.CFG). The example files provided in Appendices B and C are internally documented. The modeled watershed outflow and the measured flow are presented for comparison in both Figs. 17.5 and 17.6. They represent *combined* model and measured values for all Lake Superior watersheds. The 20 output files in Appendix C (OUTPUT01.SUP ... OUTPUT22.SUP) are combined through the use of program "AggregateModelResults.F95," also found in Appendix C, into file OUTPUTDM.SUP.

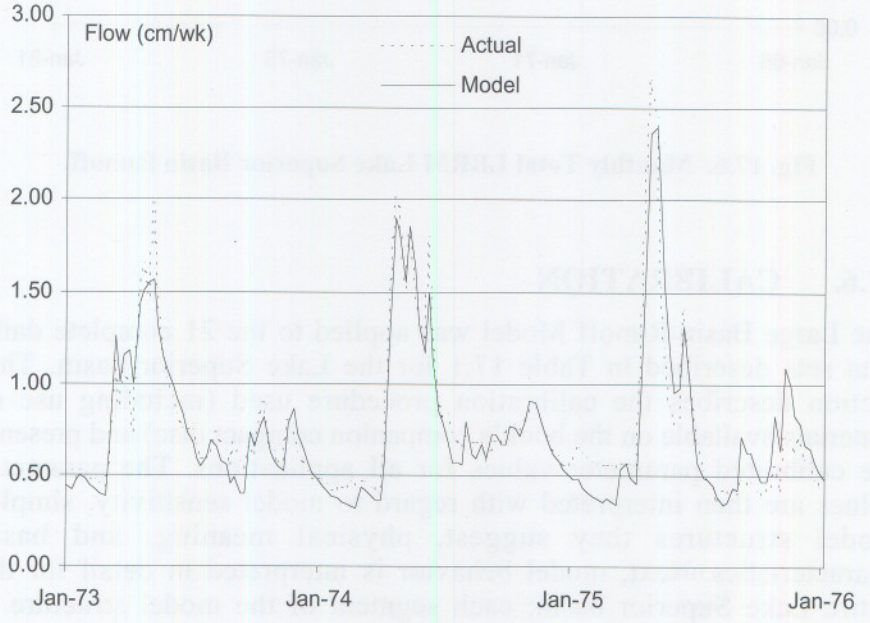

Fig. 17.5. Weekly Total LBRM Lake Superior Basin Runoff.

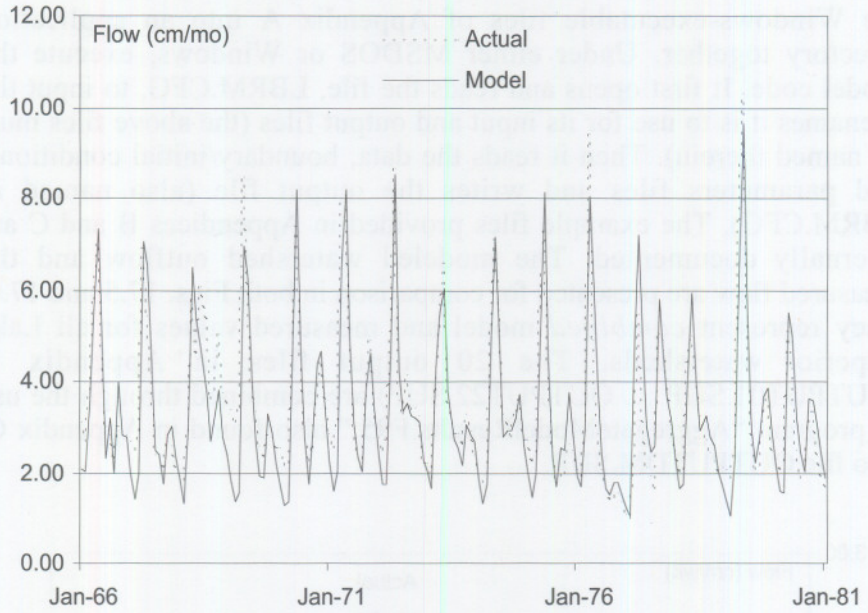

Fig. 17.6. Monthly Total LBRM Lake Superior Basin Runoff.

17.6. CALIBRATION

The Large Basin Runoff Model was applied to the 21 complete daily data sets described in Table 17.1 for the Lake Superior basin. This section describes the calibration procedure used (including use of materials available on the book's companion compact disc) and presents the calibrated parameter values for all applications. The parameter values are then interpreted with regard to model sensitivity, simpler model structures they suggest, physical meaning, and basin characteristics. Next, model behavior is interpreted in detail for the entire Lake Superior basin; each segment of the model structure is considered individually. Finally, problems inherent in the calibration procedure are discussed and improvements are suggested.

Table 17.1. Lake Superior watershed flow data availability.

Sub-Basin (1)	Basin Area (km^2) (2)	Data First Date (d/m/y) (3)	Data Last Date (d/m/y) (4)	Model Start Date (d/m/y) (5)	Calibrate Start Date (d/m/y) (6)	Calibrate End Date (d/m/y) (7)
1	9,707	1/1/48	31/12/95	1/1/48	1/1/50	31/12/95
2	4,943	1/1/42	30/9/97	1/1/48	1/10/73[a]	31/12/95
3	3,427	31/7/14	30/9/97	1/1/48	1/1/50	31/12/95
4	2,655	1/3/45	20/10/82	1/1/48	1/1/50	20/10/82
5	3,582	1/6/42	30/9/97	1/1/48	1/1/50	31/12/95
6	2,854	1/10/66	30/9/97	1/1/48	1/10/66	31/12/95
7	1,786	1/2/32	30/9/97	1/1/48	1/1/50	31/12/95
8	2,438	1/7/61	30/11/86	1/1/48	1/7/61	30/11/86
9	3,109	-	-			
10	2,130	7/8/53	30/9/97	1/1/48	7/8/53	31/12/95
11	864	-	-			
12	5,064	24/10/67	31/12/95	1/1/48	24/10/67	31/12/95
13	5,695	1/10/35	31/12/95	1/1/48	1/1/50	31/12/95
14	9,832	16/7/20	31/12/95	1/1/48	1/1/50	31/12/95
15	7,901	1/10/59	31/12/95	1/1/48	1/10/59	31/12/95
16	6,874	6/2/70	31/12/95	1/1/48	6/2/70	31/12/95
17	5,226	1/1/70	31/12/95	1/1/48	1/1/70	31/12/95
18	1,839	9/10/74	12/10/94	1/1/48	9/10/74	12/10/94
19	25,258	23/5/50	31/12/94	1/1/48	23/5/50	31/12/94
20	5,858	1/1/71	31/12/95	1/1/48	1/1/71	31/12/95
21	8,837	21/4/26	31/12/95	1/1/48	1/1/50	31/12/95
22	8,205	1/6/21	30/9/97	1/1/48	1/1/50	30/9/97
L[b]	128,084			1/1/48	1/1/50	31/12/95

[a]A gage was added on this date.
[b]Lumped application over all Lake Superior land area.

17.6.1. Calibration Procedures

Parameters are determined by a systematic search of the parameter space to minimize the root-mean-squared-error between actual daily outflow volumes, Q, and model outflow volumes, V_o,

$$\sqrt{\overline{e^2}} = \sqrt{\frac{1}{n}\sum_{i=1}^{n}\left(Q_i - \left(V_o\right)_i\right)^2} \tag{17.60}$$

where $\sqrt{\overline{e^2}}$ is root mean square error, n is the number of days for which there are flow measurements, and the subscript i refers to days. The search consists of minimizing this error for each parameter, selected in rotation, until convergence in all parameters to two or three significant figures is achieved. This procedure is implemented in FORTRAN 95 for (IBM compatible) personal computers, suitable for use under either MSDOS or Windows (95, 98, NT, or 2000). The software can also be modified to maximize sample correlation between actual and model daily flow volumes.

$$\hat{\rho} = \frac{\frac{1}{n}\sum_{i=1}^{n} Q_i\left(V_o\right)_i - \overline{Q}\,\overline{V}_o}{\sqrt{\frac{1}{n}\sum_{i=1}^{n}\left(Q_i - \overline{Q}\right)^2}\sqrt{\frac{1}{n}\sum_{i=1}^{n}\left(\left(V_o\right)_i - \overline{V}_o\right)^2}}$$

$$\overline{Q} = \frac{1}{n}\sum_{i=1}^{n} Q_i \tag{17.61}$$

$$\overline{V}_o = \frac{1}{n}\sum_{i=1}^{n}\left(V_o\right)_i$$

where $\hat{\rho}$ is sample correlation, Q is sample mean actual daily flow, and V_o is sample mean model daily outflow volume.

Appendices D - F on the book's companion compact disc for this chapter contain programs and example application information for two versions of the calibration software (DOS and Windows). (Again, all material in the appendices is available on the World Wide Web at http://www.glerl.noaa.gov/wr/lbrmexamples.html.) Appendix D, in conjunction with the files in Appendix A, provide complete source code, as well as executable files, for calibration of the Large Basin

Runoff Model using daily hydrometeorological data. Appendix E

contains an example set of additional input files (*beginning* model parameters and measured runoff) for each of the Lake Superior watersheds (see Fig. 17.4) and an example input filename list; the remaining required input files (meteorological data and boundary conditions) are present in Appendix B. Appendix F (subdirectory "DOS Calibrations") contains the corresponding ending parameter files and a log of the calibration searches, obtained through use of the DOS calibration program, DOScalib.EXE. Appendix F (subdirectory "WIN Calibrations") contains the corresponding ending parameter files, obtained through use of the Windows calibration program, WINcalib.EXE. (Note that all of these parameter files are not necessarily the same as those used in Appendix B for the example in Appendix C. This is because the Appendix F results were obtained by uninterrupted running of the calibration programs, while the parameter files of Appendix B were derived through additional experimentation.)

The model parameters are fully documented in the example files, (see, e.g., PARAM01.SUP), contained in Appendix E. The user must supply starting values as shown there. Note that the watershed area (km^2), mid-monthly daily surface insolation for each month (langleys), the linear coefficients relating the ratio of cloudy insolation/cloudless insolation to "cloud cover," and upper soil zone capacity must be entered for the watershed in question. The nine parameters and their limits are set to their initial values to begin the search (calibration) and the constant ("Cons") is set to zero. Finally, the last entry in file PARAM01.SUP in Appendix E (representing the starting parameter number to be used in the calibration) should be set to 1, 2, or 3 (to force the recomputation of "Cons" immediately); the recommended setting is "3" to allow the calibration to consider parameters 3 through 9 before it considers parameters 1 and 2.

To calibrate, place five of the files from Appendices B and E (e.g., CLMASC01.SUP and BNDCNDXX.SUP from Appendix B, and PARAM01.SUP, LBRM.CFG, and SUP01.CM from Appendix E) and either the DOS-executable or Windows-executable files of Appendix D into an application directory together. Execute the calibration code. It first opens and reads the file, "LBRM.CFG," which must name all of the files appropriately, to input the filenames it is to use for its input and output files. (These filenames can include pathnames if the files are not in the same directory as the calibration program.) Then it reads the data, boundary/initial conditions, actual flow, and initial parameters files and begins calibrating. Each line printed on the monitor (under DOS) should

agree with those contained in file CALIBRATION.LOG and upon completion, the program will write a line to the file CALIBLOG.TXT, both of which are found in the Appendix F subdirectory "DOS Calibrations." The final version of the parameter file (PARAM01.SUP) should also agree with the Appendix F subdirectory "DOS Calibrations." Final versions of the parameter files, produced with the Windows version of the calibration, should agree with the Appendix F subdirectory "WIN Calibrations."

17.6.2. Parameter Interpretations

The example model parameters of Appendix B are presented in Table 17.2 for the Lake Superior watersheds and for the entire land basin. Inspection of Table 17.2 suggests some interesting parameter interpretations. The value of T_b (the scaling parameter for air temperature used in the computation of heat available for evapotranspiration) is relatively large for watersheds 2 - 5, 7, 10 - 15, 17, and 18, indicating that for these watersheds evapotranspiration is relatively insensitive to air temperature as modeled here. It is difficult to discern the reason, as clear evidence is not available since there are regulated flows in these basins. The melt factors in column 3 of Table 17.2 are very near expected (0.2 - 0.3 cm $°d^{-1}$) with slightly higher values on watersheds 12, 13, 14, and 19. Watersheds 12, 13, and 14 are east of Lake Superior and subject to the lake effect with warmer, more humid air passing over them than other watersheds. When humidity is high, the air can carry more heat at the same air temperature than when it is low, and hence, more snowmelt per degree-day can be expected from watersheds 12, 13, and 14. Watershed 19 contains large Lake Nipigon and water flows are highly regulated, obscuring physical interpretation.

Table 17.3 provides some of the statistics of the calibrations. Inspection of the linear reservoir and evapotranspiration coefficients in Table 17.2 and the statistics in Table 17.3 suggests that some Lake Superior watersheds could be modeled more simply, i.e., with fewer storage tanks. For example, column 4 in Table 17.2 shows that watersheds 8, 13, 14, and 15 have relatively large percolation coefficients, indicating water passes quickly through the upper soil zone and storage there is small. Likewise, column 11 in Table 17.3 shows

Table 17.2. Lake Superior watersheds model parameters[a].

No.	T_b °C	a cm °d^{-1}	α_p	β_u m^{-3}	α_i d^{-1}	α_d d^{-1}	β_- m^{-3}	α_g d^{-1}	α_s d^{-1}
(1)	(2)	(3)	(4)	(5)	(6)	(7)	(8)	(9)	(10)
1	.205+1	.217+0	.421+0	.962–2	.419–2	.393–4	.780–6	.601+1	.800–1
2	.486+1	.214+0	.835+0	.304–7	.225–1	.900–7	.273–8	.100+1	.268+0
3	.560+1	.218+0	.142+1	.891–7	.268–1	.296–1	.228–7	.294–1	.284+0
4	.585+1	.239+0	.701+0	.791–7	.169–1	.699–6	.258–8	.100+1	.225+0
5	.559+1	.255+0	.128+1	.972–7	.101–1	.791–7	.822–9	.100+1	.281+0
6	.336+1	.282+0	.692+0	.194+1	.109–3	.348+0	.318+1	.390–1	.445+0
7	.492+1	.167+0	.475+0	.105–6	.171–5	.133–1	.255–8	.639+0	.153+0
8	.320+1	.207+0	.162+2	.167+2	.504–2	.714–1	.614+0	.101–2	.653+0
10	.415+1	.241+0	.368+0	.787–7	.930–4	.159–1	.911+0	.371+3	.671–1
12	.878+1	.304+0	.115+1	.541–7	.151–4	.275–1	.929–9	.800+3	.183+0
13	.671+1	.376+0	.902+9	.710–2	.500–2	.405–2	.373–9	.367–2	.170+1
14	.637+1	.338+0	.201+2	.212–7	.780–2	.608–2	.379–9	.294–2	.153+0
15	.755+1	.214+0	.100+3	.281–5	.251–1	.458–2	.279–9	.690+3	.122+0
16	.172+1	.210+0	.344+0	.157+3	.382–6	.230–2	.749+1	.108+0	.715–1
17	.423+1	.180+0	.422+0	.212–7	.485–2	.701–2	.118–8	.911+4	.778–1
18	.515+1	.159+0	.406+0	.577–7	.400–6	.242–1	.179–8	.900+3	.152+0
19	.995+0	.368+1	.162+0	.802–3	.267–3	.293–3	.941+1	.381–2	.227–2
20	.330+1	.166+0	.443+0	.561–7	.399–2	.633–7	.486–7	.800–1	.342–1
21	.283+1	.229+0	.465+1	.672–8	.337–2	.178–2	.320–9	.515–2	.108+0
22	.353+1	.149+0	.429+0	.377–7	.698–4	.912–1	.760–6	.373–1	.146+0
L[b]	.153+1	.266+0	.220+1	.965–1	.270–2	.935–2	.591–7	.286–2	.790–1

[a]The heat constant is derived from the other parameters via Eq. (17.56). The upper soil zone capacity is arbitrarily set at 2 cm. Scientific notation is used with a 3–digit mantissa and a 1–digit exponent.

[b]Lumped application wherein all Lake Superior land area is treated as one watershed.

Table 17.3. Lake Superior Watershed Calibrated Model Statistics.

No.	$\sqrt{\rho}$	$\sqrt{\overline{e^2}}$	Ratio of Averages						Average Storages[a]			
			$\frac{\overline{V}_o}{\overline{Q}}$	$\frac{\overline{V}_r}{\overline{V}_s}$	$\frac{\overline{V}_i}{\overline{V}_s}$	$\frac{\overline{V}_g}{\overline{V}_s}$	$\frac{\overline{E}_u}{\overline{V}_s}$	$\frac{\overline{E}_\ell}{\overline{V}_s}$	$\overline{S}$	$\overline{U}$	$\overline{L}$	$\overline{G}$
		cm							cm	cm	cm	cm
(1)	(2)	(3)	(4)	(5)	(6)	(7)	(8)	(9)	(10)	(11)	(12)	(13)
1	.82	.048	.98	.25	.10	.00	.40	.24	.880+0	.164+0	.475+1	.311–4
2	.78	.085	.98	.24	.20	.00	.30	.25	.375+0	.117+0	.206+1	.186–6
3	.83	.071	.97	.19	.10	.11	.32	.29	.330+0	.799–1	.848+0	.853+0
4	.86	.081	1.0	.26	.18	.00	.36	.20	.495+0	.135+0	.272+1	.190–5
5	.82	.067	.96	.19	.22	.00	.37	.23	.340+0	.812–1	.506+1	.400–6
6	.83	.140	.94	.27	.00	.32	.32	.09	.303+0	.134+0	.210+0	.185+1
7	.83	.072	.96	.28	.00	.19	.36	.17	.720+0	.173+0	.326+1	.678–1
8	.49	.059	1.0	.03	.03	.39	.29	.23	.163+0	.962–2	.134+1	.911+2
10	.91	.047	.95	.35	.00	.11	.24	.30	.157+1	.250+0	.152+1	.648–4
12	.88	.101	1.0	.25	.00	.26	.33	.17	.817+0	.108+0	.278+1	.954–4
13	.42	.079	.98	.00	.25	.20	.00	.54	.733–1	.304–9	.138+2	.152+2
14	.66	.054	.98	.04	.24	.18	.06	.48	.761+0	.114–1	.771+1	.159+2
15	.87	.051	.99	.01	.37	.07	.39	.17	.851+0	.143–2	.346+1	.230–4
16	.88	.063	1.0	.39	.00	.08	.22	.32	.149+1	.261+0	.768+1	.163+0
17	.88	.057	1.0	.33	.07	.10	.30	.20	.143+1	.194+0	.312+1	.240–5
18	.86	.080	1.0	.32	.00	.23	.33	.12	.801+0	.188+0	.209+1	.562–4
19	.33	.036	1.0	.56	.02	.02	.05	.35	.549+2	.498+0	.155+2	.117+1
20	.89	.034	1.0	.31	.07	.00	.28	.34	.225+1	.190+0	.340+1	.269–5
21	.71	.042	1.0	.11	.19	.10	.06	.54	.762+0	.364–1	.118+2	.405+1
22	.88	.060	1.0	.28	.00	.17	.33	.22	.611+0	.182+0	.364+0	.887+0
L[b]	.84	.033	1.0	.13	.08	.27	.27	.25	.137+1	.619–1	.659+1	.214+2

[a]Scientific notation is used for average storages with a 3-digit mantissa and a 1-digit exponent.

[b]Lumped application wherein all Lake Superior land area is treated as one watershed.

relatively little average storage in this zone for these watersheds; column 5 in Table 17.3 also reflects this small storage with very little surface runoff for these watersheds.

The lower soil zone is a little different. Column 7 in Table 17.2 reveals no large deep percolation coefficients, which in turn implies that

water does not pass as quickly through the lower soil zone as it does in some cases for the upper soil zone. This is also reflected in column 12 of Table 17.3, which shows significantly greater than zero average storage in the lower soil zones for all watersheds. On the other hand, interflow from the lower soil zone to the surface storage tank does vary from watershed to watershed. Calibrations for watersheds 6, 7, 10, 12, 16, 18, and 22 show the interflow coefficient is relatively very small in column 6 of Table 17.2, indicating that effectively no interflow is modeled for these watersheds. This is also reflected in column 6 of Table 17.3, which also shows almost no interflow occurs for these watersheds.

The groundwater zone can be interpreted similarly. First, to look at examples of very little groundwater storage, column 9 of Table 17.2 shows relatively large groundwater coefficients for watersheds 1, 2, 4, 5, 10, 12, 15, 17, and 18. Column 13 of Table 17.3 shows the corresponding low average groundwater storage for these watersheds, as well as watershed 20. But Table 17.2 does not show a relatively large groundwater coefficient for watershed 20; however, it does show the smallest deep percolation coefficient of any watershed. This implies very little water enters the groundwater zone (is stored in the groundwater zone) in the first place, so that the groundwater coefficient has little meaning. (This is also true for watersheds 2, 4, 5, and, to a lesser extent, 1, also with very small deep percolation coefficients) Second, to look at small groundwater flows, inspection of column 7 in Table 17.3 reveals that watersheds 1, 2, 4, 5, 19, and 20 all have relatively very small groundwater flow from storage into the surface storage. Watersheds 1, 2, 4, 5, and 20 are easily understood, as those watersheds have almost no water entering the groundwater storage in the first place (have relatively very small deep percolation coefficients). Third, to look at examples of relatively large groundwater storage, column 9 in Table 17.2 shows the smallest groundwater coefficients for watersheds 8, 13, 14, and 21, and column 13 in Table 17.3 shows correspondingly large relative average groundwater storages.

Further interpreting the large groundwater storage for watersheds 8, 13, 14, and 21 is really unnecessary here as those watershed groundwater storages are not excessive. However, sometimes very large groundwater storages may result from parameter calibration when in fact large storages are not expected from inspection of the hydrology. An example can be seen in the parameter file for watershed 21 in Appendix F, subdirectory "DOS Calibrations" (PARAM21.SUP). There

the groundwater coefficient is 0.200e–4 d^{-1}, which would imply *very* large average groundwater storage with water being stored in the groundwater zone over the long term. This could be a numerical compensation for insufficient modeling ability with regard to evapotranspiration or deep (interbasin) groundwater flow for such watersheds. Water that should have been removed from the watershed by evapotranspiration or interbasin groundwater flow, but was not, is being stored so it does not appear eventually in the watershed outflow. Or, this could be a result of flow measurement inconsistencies. Inspection of the flow records for watershed 21 reveal changes in flow variability that probably correspond to changes in the flow gage network. Or, this could be a result of actual groundwater storage behavior. Inspection of the flow records for watershed 14 reveal a slightly (but slowly) increasing trend in measured flows that is duplicated in the model. Normally, one does not expect much groundwater storage on the watersheds surrounding Lake Superior, as those basins rest on the Canadian shield with only shallow soil depths upon bedrock. Observations such as these are the basis for continued parameter calibration experimentation and point out the need for the modeler to interpret the results carefully. The parameter calibration procedure does not give unique results, and alternative starting values yield different final values for the parameter sets. This was the case here and continued experimentation was used to find the parameter sets of Appendix B after those of Appendix F were first derived.

The surface storages on all watersheds behave much more uniformly than the other storages. As can be seen in column 10 of Table 17.2 and column 10 of Table 17.3, relatively small coefficients correspond to relatively large average storages and vice-versa. The largest surface coefficient and the correspondingly smallest average surface storage on any of the watersheds occurs in watershed 13, which can be seen in Fig. 17.4 to be the narrowest watershed draining into Lake Superior. The smallest surface coefficient and the correspondingly largest average surface storage on any of the watersheds occurs in watershed 19. It is interesting to note that the presence of Lake Nipigon, a large lake, in watershed 19 corresponds to this largest surface storage in all of the watershed model applications. Finally, evapotranspiration appears to come predominantly from the upper soil zone on most watersheds; exceptions shown in columns 8 and 9 in Table 17.3 occur for watersheds 10, 13, 14, 16, 19, 20, and 21.

The root-mean-square-error and correlation for these model applications allow comparison between "natural" watersheds (where there is little or no man-made flow regulations, diversions, or other changes to the natural flows) and "non-natural" watersheds (where there is). The model performs noticeably better for a watershed with only natural flow since diversions and regulations of flows are not represented in the model. Flows from watershed 10 are unaffected by man and it yields the best model correlation among all watersheds, while still maintaining a small root-mean-square-error. In contrast, goodness-of-fit values are not as good for watersheds 8 and 19. Flow regulations in watershed 8 result in frequent changes of outflow amounting to over two orders of magnitude in a single day; this prohibits effective calibration. The Ogoki diversion and regulation of outflow from Lake Nipigon for hydropower purposes both affect watershed 19.

Table 17.4 contains storage half-lives for the lumped-parameter application to the entire Lake Superior basin (land portion treated as one watershed), indicated as the last row in Tables 17.2 and 17.3 labeled

Table 17.4. Lake Superior lumped-application half-lives.

Upper Soil Zone Storage Half-Life[a]	Lower Soil Zone Storage Half-Life[a]	Groundwater Zone Storage Half-Life	Surface Zone Storage Half-Life
7.6 h	8.2 w	34.6 w	8.8 d

[a]Uncorrected for evapotranspiration.

"L." The half-lives in Table 17.4 were computed similarly to Eq. (17.12) but using the sum of all linear reservoir coefficients for a storage zone, and are uncorrected for evapotranspiration; see Croley and Hartmann (1983). The surface zone storage half-life is larger than that of the entire Lake Ontario basin (Croley and Hartmann, 1983) and may reflect the boggy, swampy nature of much of the Lake Superior basin. The groundwater zone storage half-life for Lake Superior is almost an order of magnitude less than the groundwater zone storage half-life for Lake Ontario, and may reflect the presence of the Precambrian shield under much of the Lake Superior basin. The upper soil zone storage

half-life is smaller than that for the Lake Ontario basin, while the lower soil zone half-life is about the same. This may imply that, for the Lake Superior basin, a single soil zone may be adequate to model the basin response. This is also consistent with the general structure of the Lake Superior basin - a thin layer of soil over bedrock.

Spatial integration effects tend to cancel model errors for small areas when the areas are added together; the entire-basin (lumped) model performs better than individual watershed models; see Table 17.3 root-mean-square-errors. Likewise, a "distributed" application may be constructed by summing the outputs from all of the watershed models spatially; the correlation and root-mean-square-error with actual flows are, respectively, 0.88 and 0.029 cm. This is even better than the lumped model. The distributed model shows better correlation and root-mean-square-error than the lumped model, undoubtedly because of the use of more information for the distributed application, which is then lost in the spatial integration of data by the lumped model.

Figure 17.7 graphically represents the storage states within the total Lake Superior watershed; it is obtained by aggregating end-of-week storages of the 20 constituent watershed models. During winter all precipitation accumulates in the snow pack and there is no net supply to the upper soil zone. Peak snow pack accumulations generally occur in March and agree with snow pack characteristics observed by Phillips and McCulloch (1972). As melt occurs in early spring, the snow pack drops quickly. The rate of disappearance of the snow pack given by the model is supported by observations by Price et al. (1976). They measured loss of water from sub-arctic snow packs up to 5.9 cm d^{-1} from densely wooded north-facing slopes. They also observed the melt season typically lasts from 7 to 27 days, depending on site characteristics and snow pack depth. The model is judged to have good snow melt timing; however, comparison with remotely-sensed snow water equivalents suggests model deficiencies regarding snow pack volumes.

As the snow pack melts quickly, the upper soil zone experiences large peaks in the net supply rate. Throughout the summer the net supply rate to the upper soil zone is strictly precipitation. Figure 17.7 also shows the modeled upper soil zone storage for the Lake Superior basin; it is typically very small since the upper soil zone is modeled to be very "flashy." Variations in the upper soil zone storage correspond directly to the net supply rate.

Peaks in the lower soil zone storage also correspond directly to the net supply rate peaks (not shown) since almost all the water percolates immediately through the upper soil zone. Clear recessions in the lower soil zone moisture are evident in winter when there is no net supply. The peak lower soil zone moisture results from the large spring snow melt influx. During summer, when evapotranspiration losses are highest,

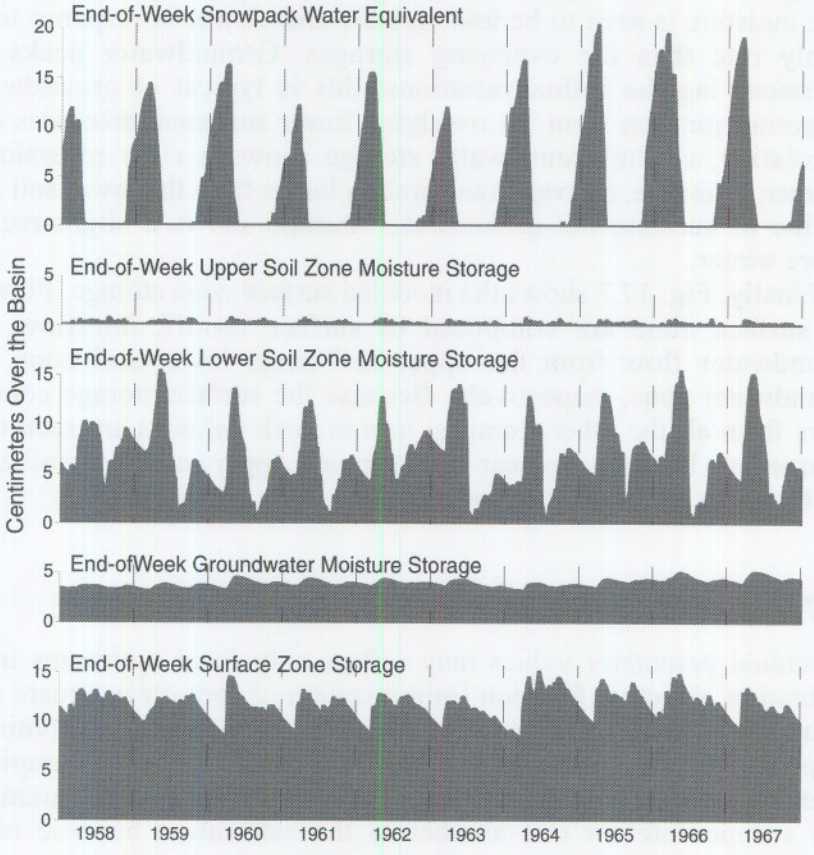

Fig. 17.7. Weekly Lake Superior Basin Moisture Storages.

the lower soil zone moisture is quickly depleted. Evapotranspiration demands become significant in May when trees and other vegetation begin to leaf out; with subsequent higher temperatures in June or July, all moisture in the lower soil zone can be removed by evapotranspiration. The continued high temperatures during the

remainder of the summer prohibit any recovery of soil moisture levels in the lower zone. Instances where the lower soil zone moisture remains relatively high throughout June are cool springs or late summers. In autumn, as average daily air temperatures decrease and plants cease production, the demands on the lower soil zone from evapotranspiration also fall and the water volume begins to rebuild.

Figure 17.7 also depicts modeled groundwater storage. Groundwater zone moisture is seen to be less variable and slower in response to net supply rate than the overlying storages. Groundwater peaks and recessions lag the influx variations; this is typical of groundwater. Evapotranspiration from the overlying lower soil zone precludes deep percolation, so the groundwater storage shows a clear recession in summer. Likewise, as evapotranspiration losses from the lower soil zone decline in autumn, the groundwater storage shows a slight recover before winter.

Finally, Fig. 17.7 shows the modeled surface zone storage. Flows to the surface zone are composed of surface runoff, interflow, and groundwater flow from the upper soil zone, lower soil zone, and groundwater zone, respectively. Because the surface storage contains flows from all the other storages, lags in peak volumes are seen to be intermediate between the near-instantaneous upper and lower soil zones and the slower groundwater zone.

17.7. CALIBRATION PROBLEMS

Individual parameter values may reflect only local optimums in the calibration objective function (minimization of root-mean-square error of model outflows). The physical relevance of the linear reservoir and evapotranspiration parameters permits verification as empirical techniques are developed. Admittedly, errors in individual parameters may compensate for one another in the calibration because of the synergistic relationship among all parameters.

17.7.1. Non-Uniqueness

Studies on the Lake Ontario Basin (Croley, 1982a, 1983b) show that the simple search algorithm described herein does not give unique optimums for calibrated parameter sets because of synergistic

relationships between parameters. However, the calibration procedure does show a high degree of repeatability for recalibrations with different starting values, and consistent parameter values are obtained for watersheds with similar hydrologic characteristics. The non-uniqueness of the calibrated parameter sets obtained for Lake Superior applications was determined following Sooroshian and Gupta (1983). The hypothesis was that, if parameter sets are unique, then parameter values produced from calibration of a synthetic data set should be identical to the parameter set used to create that synthetic data set. The model was first calibrated to the lumped data set (identified as "L" in Tables 17.1, 17.2, and 17.3). The model was then used with these calibrated parameters to generate outflows for a new calibration. Subsequent calibration started with a very different initial parameter set and yielded a different optimum parameter set with a relatively poor goodness-of-fit, illustrating the non-uniqueness of the parameters, the importance of the starting values used in the search, and the problems inherent in searching the parameter space.

17.7.2. Realism

Sooroshian and Gupta (1983) have identified three causes of problems in determining unique and realistic parameter values through calibration: 1) model structure representation, 2) data and their associated measurement errors, and 3) imperfect representation of the real world physical processes by the model. Model structures that include threshold parameters may require search algorithms unable to find the "true" optimum; hence, the calibration may fail to find the "'true" optimum for other parameters. The runoff model described herein contains no threshold parameters.

Errors associated with the measurement of input data (e.g., precipitation, air temperature, insolation, streamflow) will reduce the quality of parameter estimation unless those errors can be filtered out. Also, if the data set used to calibrate the parameters does not adequately represent the entire range of possible events, some model storages or processes may be activated too infrequently for a meaningful parameter determination. However, use of more data may not be the best solution; Sooroshian et al. (1983) show that use of long calibration data sets is not as important as the use of data sets with adequate hydrologic variability. They suggest that the use of "wet years" is more likely to sufficiently

activate all parameters so that realistic parameter values are obtained. Sooroshian (1983) also cautions that, when excessively long data sets are used for calibration, data "noise" interpreted as valid information may result in "over-fitting" of the model.

Rainfall-runoff models certainly are simplifications of actual hydrologic processes. Time-invariant parameters, such as snow albedo (used in application of the model to the Lake Ontario basin), are unlikely to represent reality. The parameters most likely to portray watershed response could actually vary seasonally or trend with time because of physical changes in the watershed, such as deforestation or urbanization. Also, lumping of spatially distributed data to represent the entire watershed can adversely affect parameter optimization. On the other hand, spatial filtering can imply that data or model errors for small areas cancel each other out as the areas are added together; this was apparent in the application of the model to both the Lake Ontario Basin (Croley and Hartmann, 1983) and the Lake Superior Basin here. Additionally, some components in a conceptual model are more likely to adequately represent their processes in the real world than others. Sooroshian and Gupta (1983) suggest that parameter estimation techniques that properly weight the more accurate parts of the model could improve parameter estimates.

17.7.3. Objective and Convergence

Sooroshian (1983) reviews additional questions concerning calibration of rainfall-runoff models, including choice of an appropriate objective function and convergence criteria. Sooroshian et al. (1983) assert that statistical measures other than root-mean-square error can result in more realistic parameter values and improved forecast performance even though the root-mean-square error criteria may provide a better fit to the calibration data. Also, parameters should be allowed to stabilize rather than depending solely on the convergence of the objective function value (e.g.. root-mean-square error) because parameter values may still change considerably. Parameter stabilization to three significant digits was used, in all Large Basin Runoff Model calibrations in lieu of convergence criteria on the objective function.

17.8. MODEL VALIDITY AND APPLICABILITY

17.8.1. Evaluation

The LBRM, calibrated earlier to 1965-82 data, was used in forecasts of Lake Superior water levels (Croley and Hartmann, 1987), and comparisons with climatic outlooks showed the model was very close to actual runoff (monthly correlations of water supply were on the order of 0.99) for the period August 1982 - December 1984 which is outside of and wetter than that calibration period (Croley and Hartmann, 1986). The model also was used to simulate flows for the time period 1956-63, outside of the period of calibration, for all of the Great Lakes. The correlations of monthly flow volumes between the model and observed during this verification period are contained in Table 17.5. They are a little lower than the calibration correlations but quite good except for Lakes Superior and Huron (there were less than two thirds as many flow gages available for 1956-63 as for the calibration period for these basins).

Table 17.5. Large Basin Runoff Model Calibration Statistics[a].

Lake	No. Water-sheds	Flow Mean (mm)[b]	Flow Std. Dev. (mm)[b]	Root Mean Square Error (mm)[b]	Correlation[c]	
					Calib.	Verif.
(1)	(2)	(3)	(4)	(5)	(6)	(7)
Superior	22	1.12	0.67	0.25	0.93	0.77
Michigan	29	0.89	0.47	0.18	0.93	0.86
Huron	27	1.06	0.69	0.26	0.92	0.69
St. Clair	7	0.90	1.36	0.62	0.89	0.87
Erie	21	1.01	1.28	0.54	0.91	0.90
Ontario	15	1.41	1.13	0.43	0.93	0.89

[a]Statistics and calibrations are 1966-83; verification is 1956-63.

[b]Equivalent depth over the land portion of the basin for monthly flows, expressed as daily statistics.

[c]Monthly correlations.

17.8.2. Comparison

Croley et al. (1996, 1998) used GLERL's LBRM to study alternative climate simulations. Although GLERL uses a daily resolution of data with their models, basin-wide processes of runoff, over-lake precipitation, and lake evaporation respond discernibly to weekly changes at best, and monthly was adequate for net supply and lake level simulation (Croley et al., 1996); this ignores short-term fluctuations associated with storm movement. Likewise, spatial resolution finer than about 1000-5000 km^2 (the present average resolution of GLERL's models and their applications) is unnecessary, for use with general circulation models (GCMs) of the atmosphere, and much can be done in assessing hydrology changes at resolutions of 100,000 - 1,000,000 km^2 with lumped versions of the models. This coarse spatial resolution is still much finer than present GCM grids.

The models were assessed partially by computing net basin supplies to the lakes (basin runoff plus overlake precipitation minus overlake evaporation) with historical meteorological data for 1951-80 and comparing to historical net basin supplies. The absolute average annual difference ranged from 1.6% to 2.7% on the deep lakes, while the Lake St. Clair and Lake Erie applications were 12.0% and 7.0% respectively; month-to-month differences showed more variation. These differences generally reflect poorer evaporation modeling on the shallow lakes and snowmelt and evapotranspiration model discrepancies for the other lake basins. While monthly differences were generally small, a few were significant. The low annual residuals were felt to be acceptable for use of these models in assessing changes from the current climate as they would be consistently applied to both a "present" and a "changed" climate. Further assessment of model deficiencies with comparisons to historical net basin supplies is difficult since the latter are derived from water budgets which incorporate all budget term errors in the derived net basin supplies.

There is some indication of model applicability outside of the time periods over which the models were calibrated as indicated above and in Table 17.5. To assess the applicability of the process models to a climate warmer than the one under which they were calibrated and verified requires access to meteorological data and process outputs for the warmer climate, which unfortunately do not exist. Warm periods

Lakes. In particular, data are lacking on watershed runoff to the lakes, water surface temperatures, wind speed, humidity, cloud cover, and solar insolation.

It is entirely possible that the models are tied somewhat to the present climate; empiricism is employed in the evapotranspiration component of the LBRM. Coefficients were determined or selected in accordance with the present climate. The models are all based on physical concepts that should be good under any climate; however, the assumption is made that they represent processes under a changed climate that are the same as the present ones. These include linear reservoir moisture storages, partial-area infiltration, lake heat-storage relations with surface temperature, and gray-body radiation. However, the calibration and verification periods for the component process models include a range of air temperatures, precipitation, and other meteorological variables that encompass much of the changes in these variables predicted for a changed climate. Even though the changes are transitory in the calibration and verification period data sets, the models appear to work well under these conditions.

SUMMARY

The Large Basin Runoff Model developed at GLERL is an accurate, fast model of weekly or monthly (derived from daily) runoff volumes from the Lake Superior watershed; it has relatively simple calibration and data requirements. Parameters have physical significance and calibrated values obtained from parameter optimizations appear reasonable. Distributed and lumped applications to the Lake Superior Basin illustrate spatial integration effects on model resolution and filtering of both information and data errors consequent with these applications. The distributed-parameter application is marginally better than the lumped-parameter application. The lumped application to the entire Lake Superior Basin yielded a correlation of 0.84 and the distributed application yielded a correlation of 0.88. Applications of the model to watersheds about Lake Superior show good-to-exceptional agreement with available flow data where flows are natural and unregulated; applications to watersheds with regulated flows varied from poor to good.

Continued investigation into parameter calibration appears warranted for determining minimum data set length requirements, the importance of hydrologic variability within the calibration data set, parameter interactions, and use of different calibration objective functions and convergence criteria. The goal should be to obtain unique parameter sets while retaining their realism. Also, continued model improvement is appropriate, especially concerning snow melt runoff volumes. However, it is unlikely that any model modifications will be able to adequately simulate the extreme variability because of regulation of flows.

The model has potential for use in predictive studies since basin storages are represented directly. Predictions are limited by available meteorological information, but forecasting is practical if near real-time data are available. Since requisite data are limited to precipitation and air temperature, these requirements are met on a continuing basis for many areas of the Great Lakes Basin and other areas of the country.

ACKNOWLEDGMENT

This is Great Lakes Environmental Research Laboratory contribution no. 1171.

REFERENCES

Barnes, B. S., 1940. Discussion of analysis of runoff characteristics. Transactions American Society of Civil Engineers 105:106.

Bouchet, R. J., 1963. Evapotranspiration reele et potentielle signification climatique, Pub. No. 62, pp. 134-142, International Association of Scientific Hydrology, General Assembly at Berkeley, University of California, Berkeley, Calif., published in Gentbrugge, Belgium.

Crawford, N. H, and R. K. Linsley, 1966. Digital simulation in hydrology: Stanford watershed model IV. Technical Report No. 39, Stanford University, Department of Civil Engineering, Stanford, Calif., July, 210 pp.

Croley, T. E., II, 1977. Hydrologic and Hydraulic Computations on Small Programmable Calculators. University of Iowa, Iowa Institute of Hydraulic Research, Iowa City, Iowa, 837 pp.

Croley, T. E., II, 1982a. Great Lakes basins runoff modeling. NOAA Technical Memorandum ERL GLERL-39, National Technical Information Service, Springfield, Va. 22161. 96 pp.

Croley, T. E., II, 1982b. A tank-cascade runoff model for large forested basins. In Proceedings of Canadian hydrology symposium '82: Hydrological Processes of Forested Areas, Associate Committee on Hydrology, National Research Council of Canada. Ottawa, Ont., 419-439.

Croley, T. E., II, 1983a. Great Lakes basins (U.S.A.-Canada) runoff modeling. Journal of Hydrology, 64:135-158.

Croley, T. E., II, 1983b. Lake Ontario basin (U.S.A.-Canada) runoff modeling. Journal of Hydrology, 66:101-121.

Croley, T. E., II, 1990. Laurentian Great Lakes double-CO2 climate change hydrological impacts. Climatic Change, 17:27-47.

Croley, T. E., II, 1992. Climate change impacts on Great Lakes water supplies. Proceedings of the Symposium on Managing Water Resources During Global Change, 28th American Water Resources Association Conference, 241-250.

Croley, T. E., II, 1993a. CCC GCM 2xCO2 hydrological impacts on the Great Lakes. In: Climate, Climate Change, Water Level Forecasting and Frequency Analysis, Supporting Documents, Volume 1 - Water Supply Scenarios, International Joint Commission, Washington, DC.

Croley, T. E., II, 1993b. Probabilistic Great Lakes hydrology outlooks. Water Resources Bulletin, 29(5):741-753.

Croley, T. E., II, and H. C. Hartmann, 1983. Lake Ontario basin runoff modeling. NOAA Technical Memorandum ERL GLERL-43, National Technical Information Service, Springfield, Va. 22161, 108 pp.

Croley, T. E., II, and H. C. Hartmann, 1984. Lake Superior basin runoff modeling. NOAA Technical Memorandum ERL GLERL-50, National Technical Information Service, Springfield.

Croley, T. E., II, and H. C. Hartmann, 1985. Resolving Thiessen polygons. Journal of Hydrology, 76:363-379.

Croley, T. E., II, and H. C. Hartmann, 1986. Near-real-time gorecasting of large-lake water supplies; a user's manual. NOAA Technical Memorandum ERL GLERL-61, Environmental Research Laboratories, Boulder, Colorado.

Croley, T. E., II, and H. C. Hartmann, 1987. Near-real-time forecasting of large lake supplies. Journal of the Water Resources Planning and Management Division, 113(6):810-823.

Croley, T. E., II, and H. C. Hartmann, 1989. Effects of climate changes on the Laurentian Great Lakes levels. In The Potential Effects of Global Climate Change on the United States: Appendix A-Water Resources, J. B. Smith and D. A. Tirpak (Eds.), U.S. Environmental Protection Agency, Washington, D.C., pp 4-1 - 4-34.

Croley, T. E., II, and D. H. Lee, 1993. Evaluation of Great Lakes net basin supply forecasts. Water Resources Bulletin, 29(2):267-282.

Croley, T. E., II, F. H. Quinn, K. E. Kunkel, and S. A. Changnon, 1996. Climate transposition effects on the Great Lakes hydrological cycle. NOAA Technical Memorandum ERL GLERL-89, Great Lakes Environmental Research Laboratory, Ann Arbor, Michigan.

Croley, T. E., II, F. H. Quinn, K. E. Kunkel, and S. A. Changnon, 1998. Great Lakes hydrology under transposed climates. Climatic Change, 38:405-433.

Derecki, J. A., and A. J. Potok, 1979. Regional runoff simulation for southeast Michigan. Water Resources Bulletin, 15(5):1418-1429.

Edson, C. G., 1951. Parameters for relating unit hydrographs to watershed characteristics. Transactions American Geophysical Union, 32:591-596.

Gauthier, R. L., R. A. Melloh, T. E. Croley II, and H. C. Hartmann, 1984. Proceedings 18th International Symposium on Remote Sensing of the Environment, Paris, pp 1-12.

Gray, D. M., 1973. Handbook on the Principles of Hydrology. Water Information Center, Manhasset Isle, Port Washington, New York, 626 pp.

Hartmann, H. C., 1990. Climate change impacts on Laurentian Great Lakes levels. Climatic Change, 17:49-67.

Kalinin, G. P., and P. I. Miljukov, 1958. Priblizhennyy raschet neustanovivshegosha dvizheniya vodnykh mass, Trudy Central'nogo instituta prognozov, 66.

Kumar, S., 1980. Incorporation of the SCS infiltration model into the IIHR watershed model. MS thesis, University of Iowa, Department of Civil and Environmental Engineering, Iowa City, Iowa, August. 207 pp.

Linsley, R. K., M. A. Kohler, and J. L. H. Paulhus, 1975. Hydrology for Engineers. Second Edition, McGraw-Hill, New York, New York, 482 pp.

Morton, F. I., 1965. Potential evaporation and river basin evaporation. Journal Hydraulics Division, 91:67-97.

Nash, J. E., 1959. Systematic determination of unit hydrograph parameters. Journal Geophysical Research, 64:111-115.

Nash, J. E., 1960. A unit hydrograph study with particular reference to British catchments. Proceedings of the Institute of Civil Engineering, 17, Institution of Civil Engineers, London, England.

Phillips, D. W., and J. A. W. McCulloch, 1972. The climate of the Great Lakes basin. Climatological Studies No. 20, Atmospheric Environment Service, Environment Canada, Toronto, Ont. 40 PP.

Potok, A. J., 1980. Evaluation of the SSARR and NWSH Models for Great Lakes Hydromet Studies. Appendix G, Hydrometeorological forecast system for the Great Lakes, US Army Corps of Engineers, Great Lakes Basin Hydromet Network Work Group, July, pp. Gl-G22.

Price, A. J., T. Dunne, and S. C. Colbeck, 1976. Energy balance and runoff from a subarctic snowpack. CRREL Report 76-27, Cold Regions Research and Engineering Laboratory, Hanover, N.H. 29 pp.

Rainville, E. D., 1964. Elementary Differential Equations. Third Edition, MacMillan, New York, New York, 521 pp.

Sooroshian, S., 1983. Surface water hydrology: on-line estimation. Review Geophysical Space Physics, 21(3):706-721.

Sooroshian, S., and V. K. Gupta, 1983. Automatic calibration of conceptual rainfall-runoff models: the question of parameter observability and uniqueness. Water Resources Research, 19(1):260-268.

Sooroshian, S., V. K. Gupta, and J. L. Fulton, 1983. Evaluation of maximum likelihood parameter estimation techniques for conceptual rainfall-runoff models: influence of calibration data variability and length on model credibility. Water Resources Research, 19(1):251-259.

Tingsanchali, T., and P. M. Loria, 1981. Sensitivity analysis of tank model parameters considered in automatic calibration. Proceedings of the International Symposium on Rainfall-Runoff Modeling, Mississippi State University, Mississippi State, Mississippi, May 18-21.

Witherspoon, D. F., 1970. A hydrologic model of the Lake Ontario drainage basin. Technical Bulletin No. 31, Inland Waters Branch, Department of Energy, Mines, and Resources, Ottawa, Canada, 12 pp.

WMO, 1975. Hydrological forecasting practices. Operational Hydrology Rept. No. 6, World Meteorological Organization, Working Group on Hydrological Forecasting of the Commission for Hydrology, pp. 37, 44, 45.

NOTATIONS

A area of the watershed (m^2)

A_w area of wetted contributing watershed portion (m^2)

a proportionality constant for snowmelt (m^3 $^oC^{-1}$ d^{-1})

b_1 empirical constant

b_2 empirical constant

C capacity of the upper soil zone (m^3)

E_g daily evapotranspiration groundwater zone volume (m^3)

E_ℓ daily evapotranspiration lower soil zone volume (m^3)

E_s daily evapotranspiration surface volume (m^3)

E_u daily evapotranspiration upper soil zone volume (m^3)

e evaporation or evapotranspiration rate (m^3 d^{-1})

e_p rate of evaporation or evapotranspiration still possible ($m^3 d^{-1}$)

f infiltration rate (m^3 d^{-1})

G content of groundwater zone (m^3)

H nonlatent heat released to the atmosphere (cal)

h degree-days per day ($^oC^{-1}$ d d^{-1})

k units and proportionality constant (cal)

L moisture content of lower soil zone (m^3)

$\bar{L}$ average daily lower soil zone moisture content (m^3)

m daily snowmelt rate (m^3 d^{-1})

m_p daily potential snowmelt rate (m^3 d^{-1})

P water content of the snow pack (m^3)

p	precipitation rate ($m^3\ d^{-1}$)
r	surface runoff rate ($m^3\ d^{-1}$)
S	content of surface storage zone (m^3)
s	daily net supply rate to the watershed surface ($m^3\ d^{-1}$)
T	air temperature (°C)
T_b	a base scaling temperature (°C)
T_{max}	maximum daily air temperature (°C)
T_{min}	minimum daily air temperature (°C)
t	time (d)
U	moisture content of upper soil zone (m^3)
$\overline{U}$	average daily upper soil zone moisture content (m^3)
V_d	daily deep percolation volume (m^3)
V_f	daily infiltration volume (m^3)
V_g	daily groundwater flow volume (m^3)
V_i	daily interflow volume (m^3)
V_o	daily basin outflow volume (m^3)
V_p	daily percolation volume (m^3)
V_r	daily surface runoff volume (m^3)
V_s	daily net supply volume (m^3)
x	ratio of hours of bright sunshine to maximum possible
Z	volume of water in storage (m^3)
z	outflow rate from a storage ($m^3\ d^{-1}$)
α	linear reservoir coefficient (d^{-1})
α_d	deep percolation coefficient (d^{-1})
α_g	groundwater coefficient (d^{-1})
α_i	interflow coefficient (d^{-1})
α_p	percolation coefficient (d^{-1})

α_s	surface outflow coefficient (d^{-1})
β	partial linear reservoir coefficient (m^{-3})
β_g	groundwater zone evapotranspiration coefficient (= 0) (m^{-3})
β_ℓ	lower zone evapotranspiration coefficient (= 0) (m^{-3})
β_s	surface zone evapotranspiration coefficient (m^{-3})
β_u	upper zone evapotranspiration coefficient (m^{-3})
γ_f	latent heat of fusion (cal g^{-1})
γ_v	latent heat of vaporization (cal g^{-1})
ρ_w	density of water (g m^{-3})
σ	daily solar insolation at the watershed surface (cal d^{-1})
τ	daily extra-terrestrial solar radiation (langleys d^{-1})
Ψ	total heat available for evapotranspiration during the day (cal)

Mathematical Models of Large Watershed Hydrology

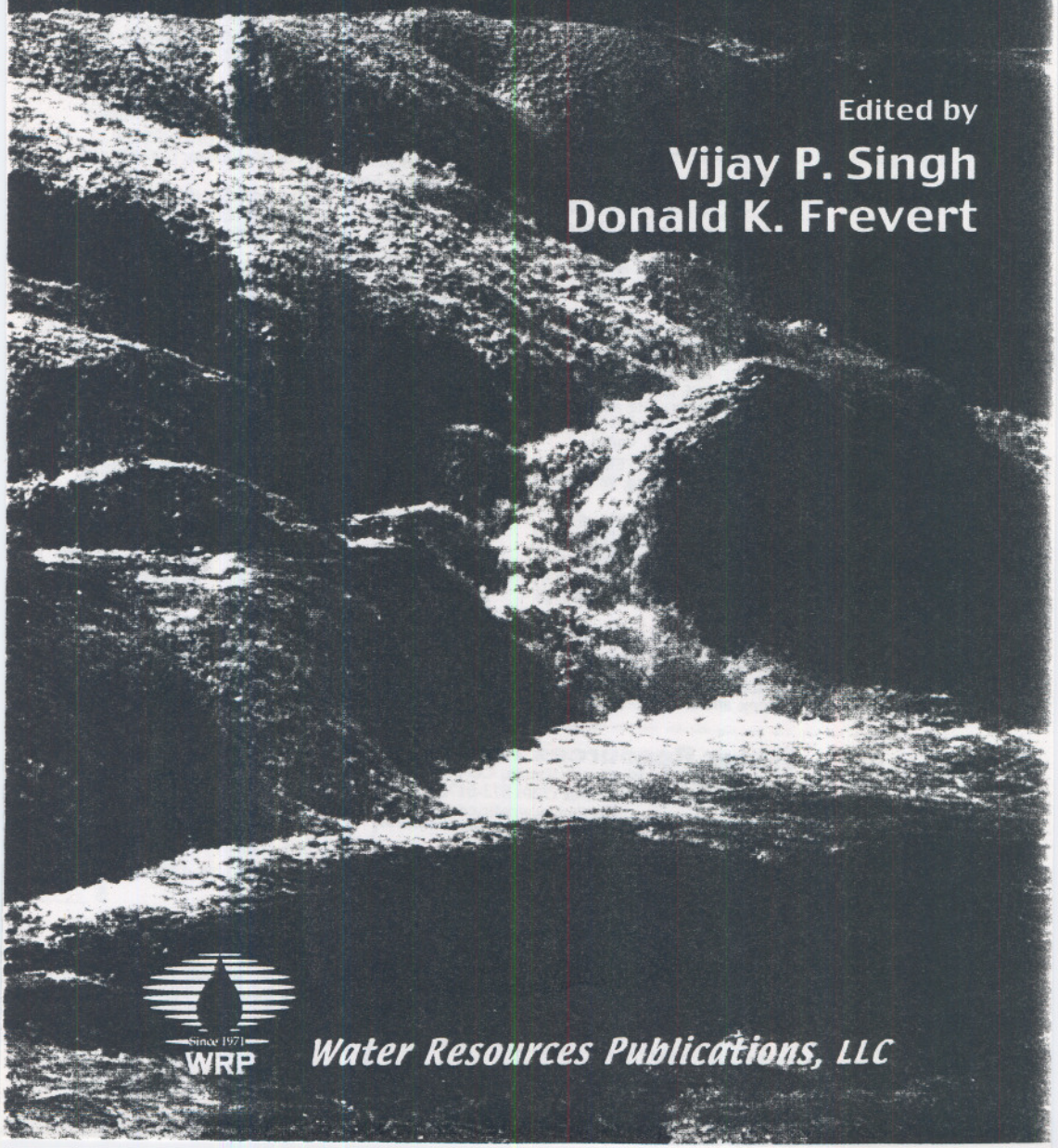

Edited by
Vijay P. Singh
Donald K. Frevert

Since 1971
WRP
Water Resources Publications, LLC

Available from Water Resources Publications, LLC

Mathematical Models of Large Watershed Hydrology

Edited by Vijay P. Singh and Donald K. Frevert

Hardcover, 914 pp, ISBN 1-887201-34-3, (Cat. No. MMLW) ~ **US $95**

Comprehensive account of some of the most popular models of watershed hydrology ~~ of interest to all hydrologic modelers and model users and a welcome and timely edition to any modeling library.

In conjunction with *Mathematical Models of Small Watershed Hydrology and Applications*, these 2 books will have a special appeal to hydrologic modelers and model users, worldwide, as well as anyone engaged in practice of hydrology, civil engineering, agricultural engineering, environmental science, forest and range science, climatology, and watershed science. Furthermore, both publications will be useful to teachers and professors who are engaged in graduate courses and research studies. Publ. 2002, WRP.

Table of Contents:

1. MATHEMATICAL MODELING OF WATERSHED HYDROLOGY ~ ***V. P. Singh and D. K. Frevert***
2. EMERGING PARADIGMS IN THE CALIBRATION OF HYDROLOGIC MODELS ~ ***L. A. Bastidas, H. V. Gupta and S. Sorooshian***
3. ANN MODELING IN WATERSHED HYDROLOGY ~ ***C. S. P. Ojha and V. P. Singh***
4. A TOOLKIT FOR THE DEVELOPMENT AND APPLICATION OF PARSIMONIOUS HYDROLOGICAL MODELS ~ ***T. Wagener, M. J. Lees and H. S. Wheater***
5. TESTING HYDROLOGIC MODELS: FORTIFICATION OR FALSIFICATION ~ ***G. Kuczera and S. W. Franks***
6. A GLOBAL HYDROLOGIC MODEL ~ ***M. L. Kavvas and M. Anderson***
7. REGIONAL-SCALE HYDROCLIMATE MODEL ~ ***J. Yoshitani, M. L. Kavvas and Z.-Q. Chen***
8. REGIONAL SIMULATION OF THE WATER BUDGET AND RIVERFLOWS WITH THE ISBA-MODCOU COUPLED MODEL: APPLICATION TO THE ADOUR AND RHONE BASINS ~ ***E. Ledoux, P. Etchevers, C. Golaz, F. Habets, J. Noilhan and S. Voirin***
9. THE HYDROLOGICAL MODELING SYSTEM ARC/EGMO ~ ***A. Becker, B. Klöcking, W. Lahmer, and B. Pfützner***
10. A STORM SIMULATION IN LARGE WATERSHEDS WITH A HYDROLOGICAL MODEL SYSTEM AND A MESOSCALE METEOROLOGICAL MODEL ~ ***Z. Yu***
11. NUMERICAL MODEL OF RIVER FLOW FORMATION FROM SMALL TO LARGE SCALE RIVER BASINS ~ ***X. Ma and Y. Fukushima***
12. THE TOPKAPI MODEL ~ ***E. Todini and L. Ciarapica***
13. CEQUEAU HYDROLOGICAL MODEL ~ ***G. Morin***
14. LASCAM: LARGE SCALE CATCHMENT MODEL ~ *M. Sivapalan, N. R. Viney, and C. Zammit*
15. WATFLOOD/SPL9: HYDROLOGICAL MODEL & FLOOD FORECASTING SYSTEM ~ ***N. Kouwen and S. F. Mousavi***
16. THE ARNO MODEL ~ ***E. Todini***
17. LARGE BASIN RUNOFF MODEL ~ ***T. E. Croley II***
18. MODELING RUNOFF FROM HYDROLOGICALLY SIMILAR AREAS ~ ***H. Koivusalo, T. Kokkonen and T. Karvonen***
19. MATHEMATICAL MODEL OF RAINFALL-RUNOFF TRANSFORMATION-WISTOO ~ ***M. Ozga-Zielinska, W. Gadek, K. Ksiazynski, E. Nachlik, and R. Szczepanek***
20. THE CLS MODEL ~ ***E. Todini***

"Some of the most popular models of watershed hydrology ~ sure to appeal to all hydrologic modelers and model users"

MathMod1
(Cat No: MM1)
US $55

Compatible CD-ROM featuring 16 modeling programs

10% Discount when ordering BOTH Book & CD-ROM

Order from: **Water Resources Publications, LLC**
P.O. Box 260026 • Highlands Ranch, CO 80163-0026 U.S.A.
Orders 1-800-736-2405 • Fax (720) 873-0173 • Info. (720) 873-0171 •
wrpllc@qwest.net • http://www.wrpllc.com

WRP

Name_____Company_____
(Please Print)
Address_____
City/State/Country_____Zip Code_____
Tel # Fax # E-mail
Credit Card Payment: ☐ Visa ☐ Mastercard
Card #_____Exp. Date___/___
Signature_____

Book (MMLW)	$ _____
CD Only (MM1)	$ _____
Book + CD (10% Disc.)	$ _____
*P/H	$ _____
TOTAL U.S.	$ _____

***Postage & Handling (P/H):**
$6 for U.S.A. -- each additional book + $2
$10 for Canada + 7% GST Tax -- each additional book + $9
All Other Countries -- Please fax or e-mail or call for quote
Colorado residents: Please add 3.8%

***For faster service** please call or fax request for quotation.